

EFFECT OF TURBULENCE ON THE HEAT TRANSFER
COEFFICIENT DISTRIBUTION AROUND A
CYLINDER NORMAL TO AIR FLOW

by

WALTER MICHAEL BOLLEN

A THESIS

submitted to


OREGON STATE COLLEGE

in partial fulfillment of
the requirements for the
degree of


MASTER OF SCIENCE

June 1949


APPROVED:




Assistant Professor of Chemical and Metallurgical
Engineering
In Charge of Major



Head of Department of Chemical and Metallurgical
Engineering



Chairman of School Graduate Committee



Dean of Graduate School

ACKNOWLEDGMENTS

The author would like to express his thanks and appreciation to Dr. J. T. Clapp, who suggested and directed the experimental work, for his help and advice on all phases of the problem.

Appreciation is also extended Professor J. S. Walton, Head of the Department of Chemical and Metallurgical Engineering, for his cooperation on the project.

Thanks are due Dr. W. B. Bollen for his general assistance and help. Also, the author would like to thank Mr. R. C. Mang, who constructed the experimental tube and turbulence indicator, and Mr. J. F. Taylor who provided the plans after which the turbulence indicator was patterned.

. . . . Thank God! there is always a Land of
Beyond

For us who are true to the trail;
A vision to seek, a beckoning peak,
A farness that never will fail;
A pride in our soul that mocks at a goal,
A manhood that irks at a bond,
And try how we will, unattainable still,
Behold it, our Land of Beyond!

Service

TABLE OF CONTENTS

	Page
INTRODUCTION	1
HISTORICAL INTRODUCTION	3
THEORETICAL CONSIDERATIONS	8
Heat Transfer	
Boundary Layer Formation	
Flow Around A Cylinder	
Nature of Turbulence	
EXPERIMENTAL PROCEDURE	17
Equipment	
Technique	
Measurement of Turbulence	
Calculations	
RESULTS AND DISCUSSION	44
CONCLUSIONS	
APPENDIX	55
Nomenclature	
Theories of turbulence	
Turbulence Determination Curves	
Bibliography	

EFFECT OF TURBULENCE ON THE HEAT TRANSFER
COEFFICIENT DISTRIBUTION AROUND A
CYLINDER NORMAL TO AIR FLOW

INTRODUCTION

The effect of turbulence on the local heat transfer coefficient distribution about a cylinder normal to an air stream was determined at two Reynolds numbers. This was deemed advisable because several previous investigators had obtained the local heat transfer coefficient variation neglecting the effect of turbulence whereas another had determined the effect of turbulence on the total coefficient.

The present investigation was carried out using a wind tunnel with a six by eighteen inch working section. Local heat transfer coefficients expressed as Nusselt numbers were determined by measuring the condensation rate of steam in sectors subtending 36 degree angles inside a two-inch copper pipe. This pipe could be rotated to expose the sectors to different positions relative to the direction of flow. It was placed normal to the air flow in the working section of the tunnel. Turbulence was generated by slats one inch wide placed on two-inch centers and mounted ten inches upstream of the experimental tube. A hot wire wake-angle instrument

was used to measure the intensity of turbulence.

The local heat transfer coefficient distribution for two Reynolds numbers and two intensities of turbulence are given by the following table.

Re No.	Turb. Level	Local Nu. No. Degrees from front of Tube			Average Nu. No.
		18°	90°	162°	
35,500	2.6%	218	126	199	168
35,500	27%	279	198	165	211
106,800	2.6%	366	325	443	360
106,800	27%	551	431	340	456

These results show that the minimum local coefficient at abnormally high turbulence occurs at the rear of the cylinder whereas the normal position for the minimum is at the side.

A short historical introduction is offered as a background for the experimental work. This is followed by discussion of the theories of heat transfer, flow about a cylinder, and the nature of turbulence. A more complete discussion of turbulence is included in the appendix. After an experimental section which includes a detailed description of the equipment, procedure, and calculations, the main results are presented and discussed. An itemized list of important observations comprises the conclusions.

HISTORICAL INTRODUCTION

Lohrisch, as early as 1926, studied the effect of fluid velocity on mass transfer to a fluid stream from local sections of a cylinder. He converted his mass transfer data to heat transfer coefficients by Colburn's heat transfer factor, j . His work indicated that the minimum Nusselt number occurred at the sides of the tube with the maximum at the front at low Reynolds numbers. With increasing Reynolds number the rear coefficient increases more rapidly than those for the front or sides, eventually becoming larger than the front coefficient. Figure 1 shows the results of Lohrisch plotted on polar coordinate paper.

Small (9) measured local temperatures in a tube wall with a thermopile from which he calculated the local heat flux and heat transfer coefficients.

Drew and Ryan (4) obtained actual heat transfer data by condensing steam inside a tube sectioned with fins. The condensate from each section was collected and measured, and from this they calculated the local heat transfer coefficient. The results obtained were similar to those of Lohrisch.

Other investigators who have studied the effect of the Reynolds number on local transfer

HEAT FLUX ABOUT A CYLINDER AS
FOUND BY LOHRISCH

4

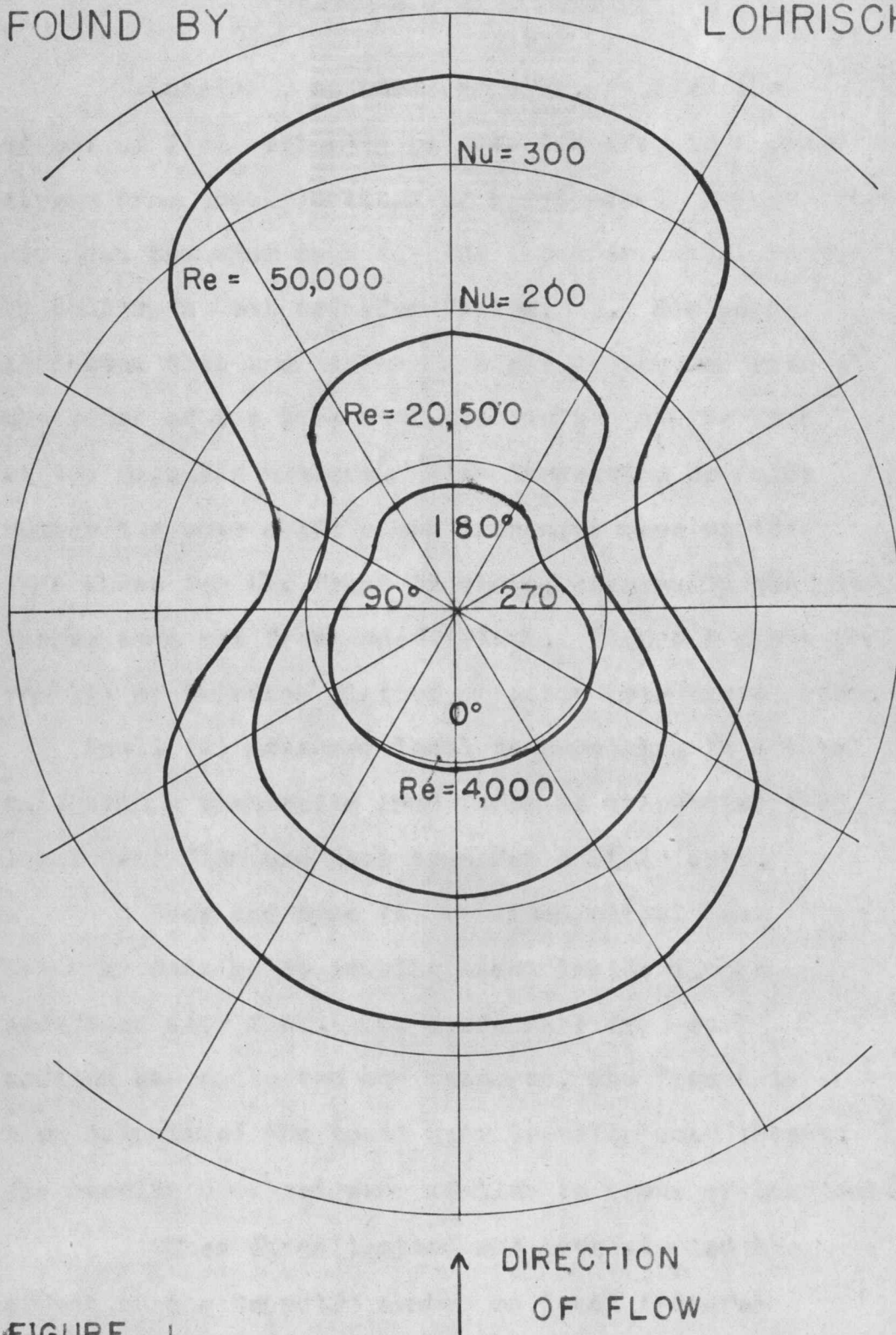


FIGURE 1

coefficients have included Winding and Cheney (10) who observed the deformation, by sublimation, of a cast naphthalene cylinder in an air stream to obtain mass transfer coefficients. These were converted to heat transfer coefficients by the j factor. This method eliminated transfer between sections, but if sufficient naphthalene is removed to allow accurate measurement of the entire tube, the shape assumed by the tube would probably alter the flow characteristics about it. The results of these workers are plotted on rectangular coordinate paper in Figure 2 for comparison.

The effect of turbulence on the overall coefficient was studied by Reiher, who passed air through a turbulence promoting grid ahead of his experimental tube. He reported increases in the overall heat transfer coefficient of 50 to 100%. Unfortunately, he did not characterize or define the turbulence produced. Comings, et. al (3 p.1077) proposed that such a large increase may have been caused by an increase in the local velocity about the tube due to a jet from the tube bundle (grid).

The work of Comings et. al (3 p.1077) showed the overall coefficient could be correlated with the turbulence of the passing stream with the equation:

HEAT TRANSFER COEFFICIENT DISTRIBUTION ABOUT A CYLINDER AS FOUND BY SEVERAL INVESTIGATORS

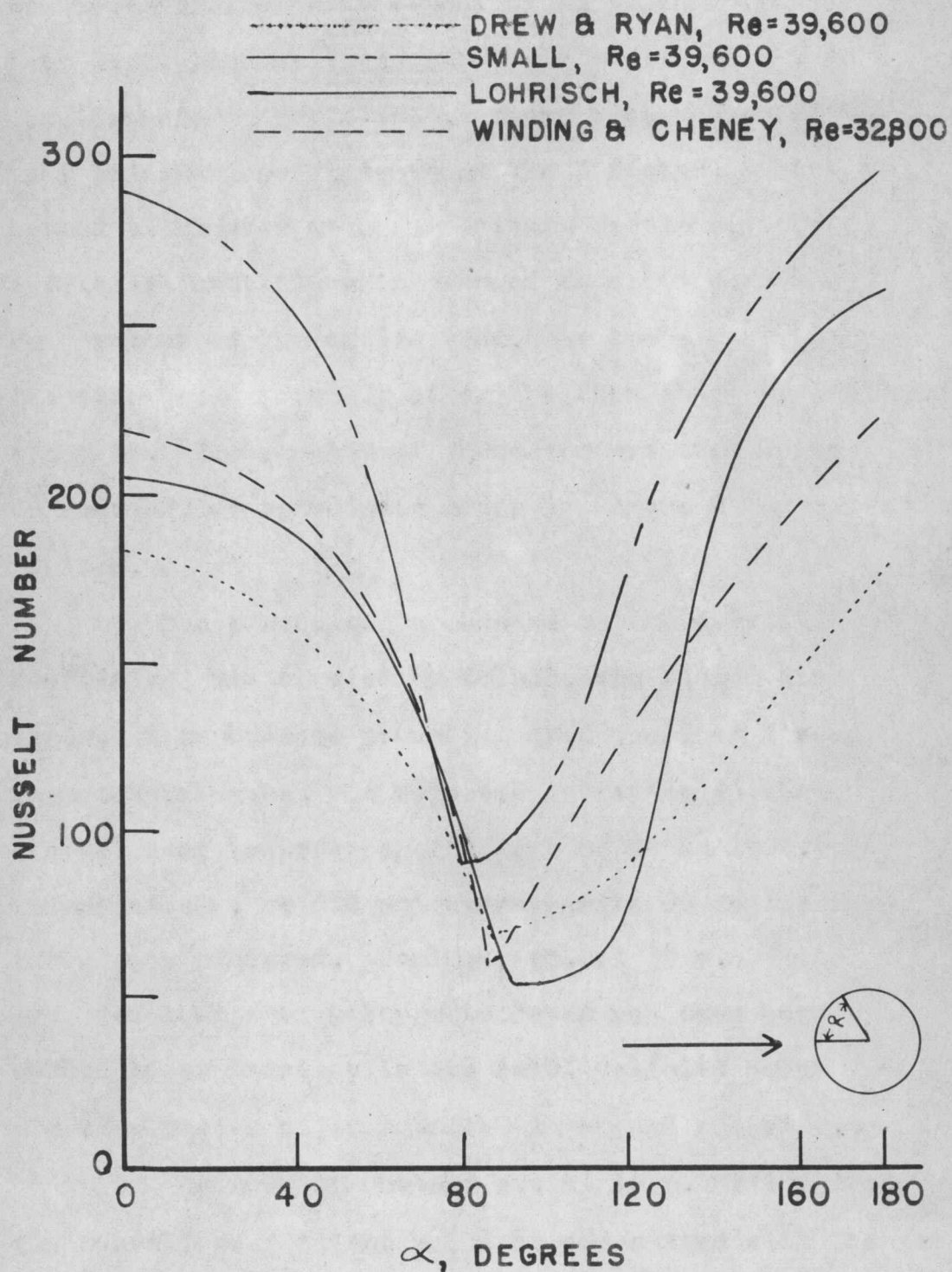


FIGURE 2

$$Nu = 25.6 \left(\frac{Re}{1750} \right)^{(0.63 - \frac{0.07}{Z})} \dots\dots\dots(1)$$

where the symbols are as shown on page 56 of the Appendix.

Note that the geometry of the turbulence generator has no bearing other than its effect on the turbulence level.

THEORETICAL CONSIDERATIONS

There are two factors to be considered in the treatment of heat transfer to a stream flowing past a tube: the transmission of heat from the condensing stream in the tube to the passing air and the nature of flow near and around the tube. The former is almost completely dependent on the latter.

Heat transfer: Considering heat transmission at any point and neglecting radiant heat for the present, the resistances affecting the rate of heat transfer for this case were the steam film, the tube wall, and the boundary layer and main stream resistance. The individual coefficients of these resistances may be combined to give the overall coefficient, U :

$$\frac{1}{U} = \frac{1}{h_s} + \frac{x}{k} + \frac{1}{h_b} \dots\dots\dots(2)$$

The values of the individual steam and tube wall coefficients are so large as compared to the local coefficients of the boundary layer that they may be neglected and the local boundary coefficient, h_b , assumed equal to U . Thus h_b at any point becomes equal to the ratio of the heat flux across the wall at that point to the total driving force between the condensing steam and the ambient air. Hence:

$$h_b = \frac{q}{A \Delta t} = \frac{\frac{q}{A}}{(t_s - t_a)} \dots\dots\dots(3)$$

The heat transferred by radiation may be expressed with the equation:

$$q_r = 0.173 A \left[\epsilon \left(\frac{T_1}{100} \right)^4 - \alpha_{12} \left(\frac{T_2}{100} \right)^4 \right] \dots(4)$$

Boundary Layer Formation: If an obstruction, such as a cylinder or a flat plate, is placed in a wind stream, it exerts a new frictional force with which the fluid must attain equilibrium. The attainment of equilibrium results in the formation of a boundary layer as conceived by Prandtl (1 p.48). This boundary layer should not be confused with the laminar film which is a permanent feature of any fully established flow pattern.

Consider a thin plate placed in the path of a uniform air stream as in Figure 3. At the front edge where the streamline abruptly contacts the edge of the plate there is a steep velocity gradient causing a large viscous force which retards the adjacent filaments. Hence a thin layer, a-a, is formed within which the viscous forces have brought about a substantial velocity change. As the stream lines move past the surface, the retarding

BOUNDARY LAYER FORMATION LAMINAR

10

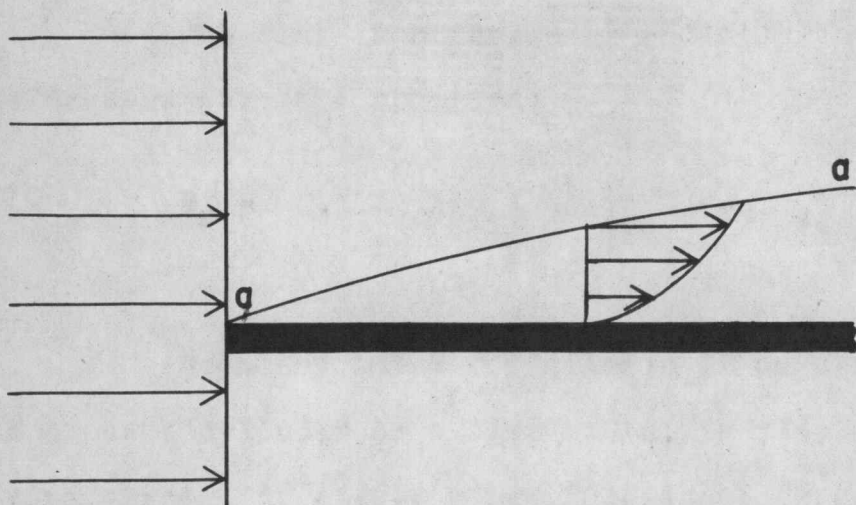


FIGURE 3

BOUNDARY LAYER FORMATION TURBULENT

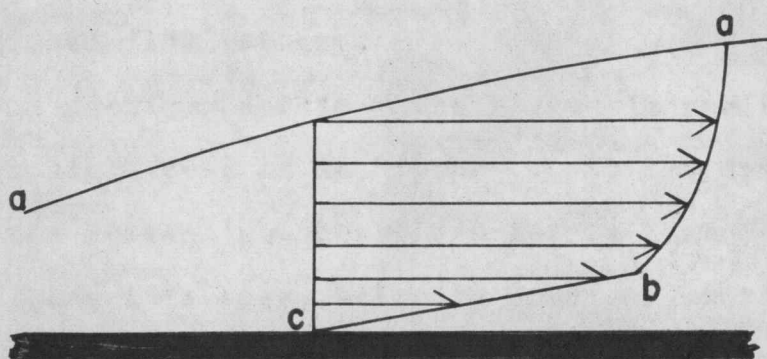


FIGURE 4

effect of the viscous forces penetrates deeper into the surrounding fluid as shown by the delimitating boundary a-a, beyond which the streamlines are practically unaffected. There is a steep velocity gradient in this boundary layer from u_a , the velocity of the main stream, to zero at the plate edge. It has been found (5 p.4) that the thickness of such a viscous layer must be of the order of magnitude of the square root of the product of kinematic viscosity and the distance from the most upstream portion divided by the square root of the air speed, i.e. $\delta = \sqrt{\frac{\nu x}{V}}$

As the thickness of the laminar layer increases, both the velocity gradient and the friction decrease to a point where the flow in the boundary layer ceases to be laminar and becomes turbulent in nature. This is illustrated in Figure 4.

The delimiting boundary is a-a, on the stream side of which the velocity remains u_0 . The velocity curve in the turbulent portion of the boundary layer is a-b, while the flow immediately adjacent to the plate continues to be laminar as exemplified by the straight line velocity curve b-c.

The point where turbulent flow in the boundary layer commences may be characterized by a dimensionless

number of the Reynolds type, $\frac{u_b x}{\nu}$ or $\frac{u_b y}{\nu}$.

Obviously, then, whether turbulent flow occurs or not, will depend on the main stream velocity, size of the obstruction in the longitudinal direction, and the kinematic viscosity of the passing fluid.

Flow around a cylinder: The same phenomena occur in flow around a cylinder as in flow past a flat plate, with the additional phenomenon of separation. As the boundary layer on a cylinder moves downstream and becomes thicker, the velocity gradient decreases and may vanish with reversal of flow occurring near the wall due to the retarding effect of pressure on the flow. This reversal causes separation of the flow from the surface and resulting burbling and turbulence around the surface from that point on downstream.

With separation, two symmetrical vortices will form directly behind the cylinder, and increase in size with increasing Reynolds number until they are swept into the downstream wake which will then consist of a series of vortex pairs. Von Karman showed such a system to be unstable, but with certain spacing* a

* When the ratio of cross stream distance between the center lines of the vortex paths to the distance between vortices in the same path equals $\frac{1}{\pi} \cos h^{-1} \sqrt{2}$
 $= 0.2806$

system of alternate vortices will be stable. The effect of the Reynolds number on such vortex formation is depicted in Figure 6 which shows sketches made from photographic studies (7 p.219) of fluid flow about a cylinder.

When the motion of the boundary layer becomes eddying, there is a more intimate mixing of the air particles, and the driving action of the outer layer on the boundary layer by momentum transfer pushes the boundary layer further along the surface before separation takes place. Obviously, then, the greater the turbulence of the main stream, the greater will be its effect upon the boundary layer separation point, pushing it further and further downstream.

Nature of Turbulence: Turbulence may be described as the fluctuation with time of the velocity at any point in a fluid stream about some mean velocity. More precisely, turbulence or intensity of turbulence is defined as the ratio of the root mean square fluctuating velocity to the mean velocity at any point.

The decay of turbulence as it progresses downstream is quite rapid, until the ratio of the distance downstream to the wire diameter of the turbulence promoter reaches about 400 (8 p.3). This is shown graphically by Figure 5. The pattern of the turbulence

DECAY OF TURBULENCE BEHIND A WIRE SCREEN

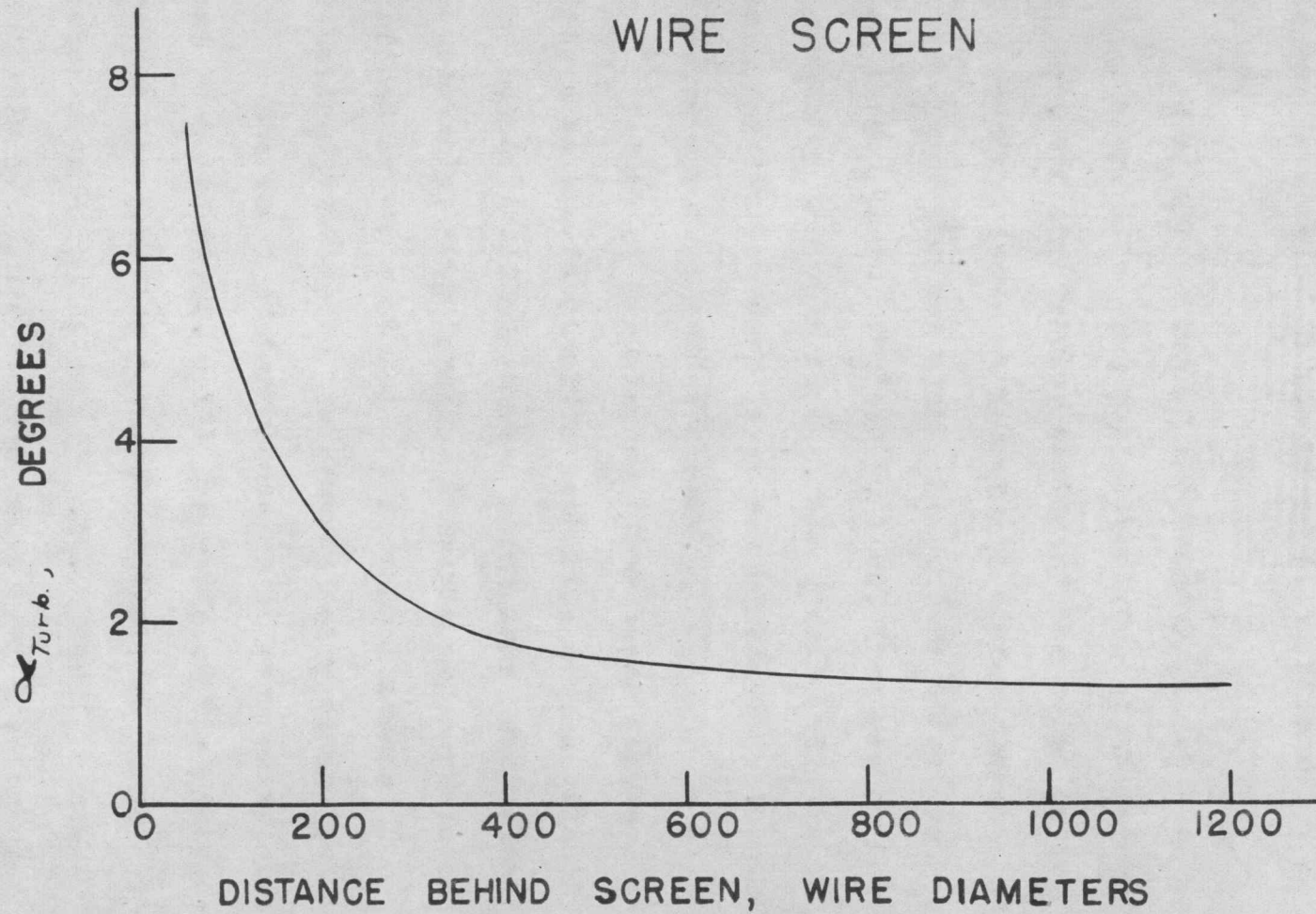
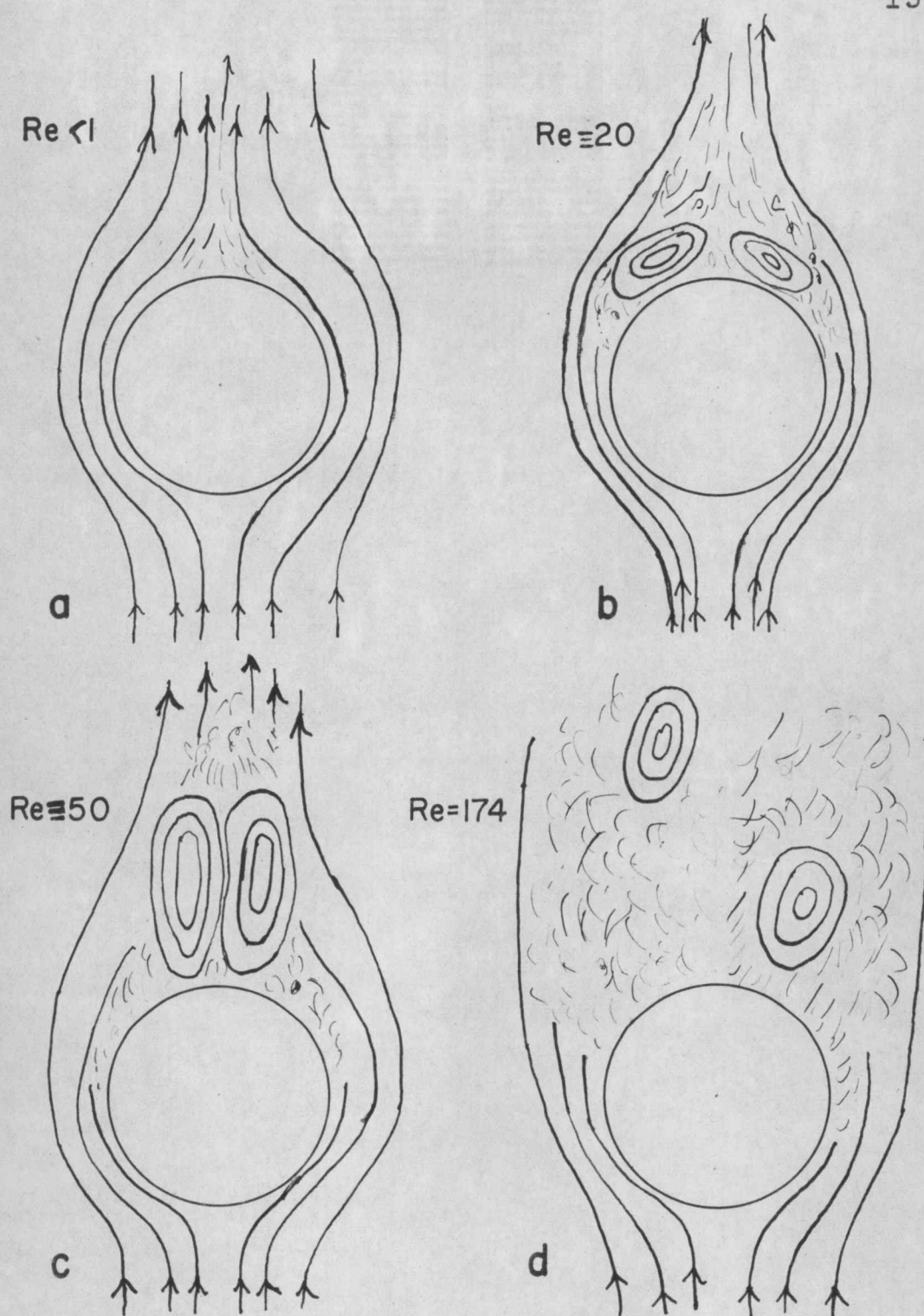


FIGURE 5



FLOW AROUND A CYLINDER WITH
INCREASING REYNOLDS NUMBER

FIGURE 6

promoting members exists downstream for about sixty-five wire diameters. Upon consideration of these two facts, it becomes apparent that abnormally high turbulence levels obtained by obstructions in an air stream are non-isotropic.

Dryden et. al. (6 p.5) define a scale factor, L, as:

$$L = \int_0^{\infty} R(y) dy$$

where R is the correlation coefficient,

$$R = \frac{v'_x v'_y}{(\overline{v'^2_x})^{1/2} (\overline{v'^2_y})^{1/2}}$$

and y is the distance between the correlated eddies. It might be noted in passing that the scale of turbulence increases with distance downstream from the grid whereas the intensity of turbulence decreases.

A more complete presentation of the theories of turbulent flow is included in the appendix.

EXPERIMENTAL

Equipment: The experimental apparatus consisted of two elements. The experimental tube with its appurtenances for determining the heat transfer coefficients, and a forced draft wind tunnel and auxiliaries for creating and characterizing a fluid flow.

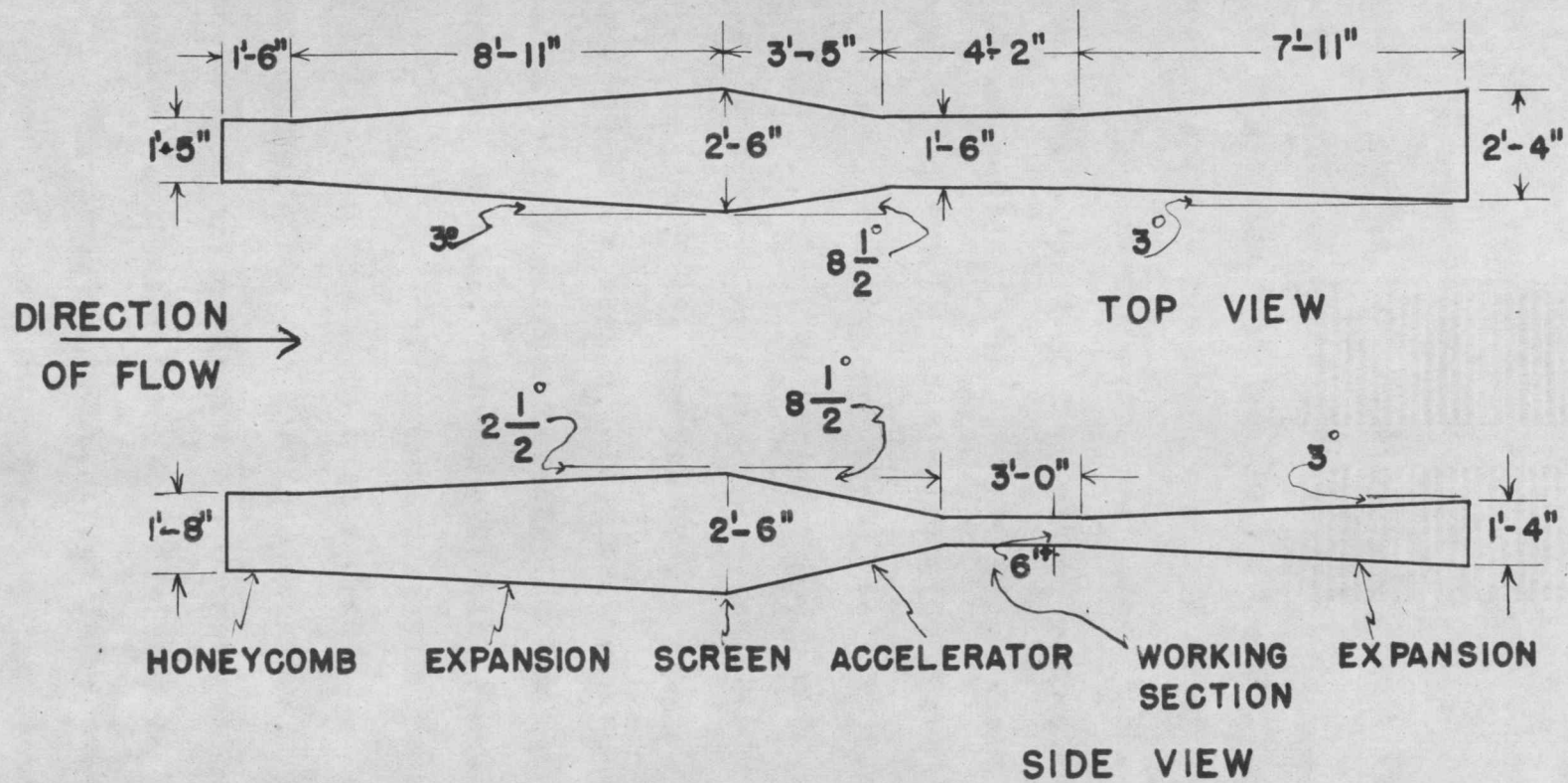
Air was supplied by an American #500E blower capable of producing 13,500 CFM at a static pressure of 6" of water gage when running at 1,255 RPM. The blower was driven by a 30 horsepower, 1,750 RPM U.S. Autostart motor. Power was transmitted by a sheave and v-belt arrangement such that the speed of the blower was 1,243 RPM when 60 cycle current was supplied. Air velocity was controlled with a sliding damper on the fan inlet.

The tunnel proper was constructed of one-half inch Douglas fir plywood in six sections for ease of handling. The ends of each section were framed with $1\frac{1}{2}$ " x 3" sash stock which served as flanges for bolting the sections together. The first section, containing a honeycomb, was an exception in that it was bolted directly to the blower through the sides, but it was flanged for connection to the next tunnel section.

The entire tunnel was supported by four standards.

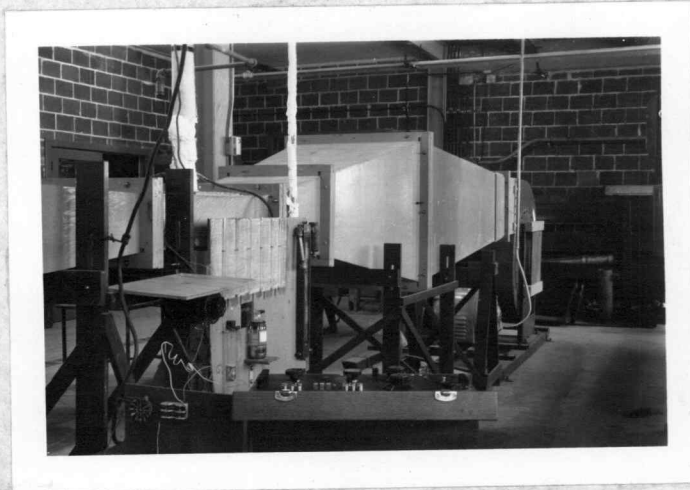
The assembled tunnel consisted of five functional parts: (1) honeycomb, (2) initial expansion section, (3) accelerator, (4) working section, and (5) final expansion section. The air first entered the honeycomb which was made up of mailing tubes one inch in diameter by eighteen inches in length. The purpose of this was to remove large swirls and eddies induced by the fan. The air then entered the initial expansion section where its velocity was decreased to about one-fifth the blower exit velocity. It then passed through a 20-mesh screen and into an accelerating section to a 6" x 18" working section. The purpose of the de-acceleration, passage through a screen, and subsequent acceleration was to provide a uniform velocity of low turbulence in the working section. From the working section the air went through the final expansion section to reduce exit losses. Figure 7 is a line drawing of the assembled tunnel giving inside dimensions. Photographs of the tunnel and equipment are mounted on pages 20 & 21. The general equipment set up is depicted in Fig. 8.

The experimental tube was fabricated from standard two-inch copper pipe, 2.06 inch inside diameter with a wall thickness of 0.158 inches.

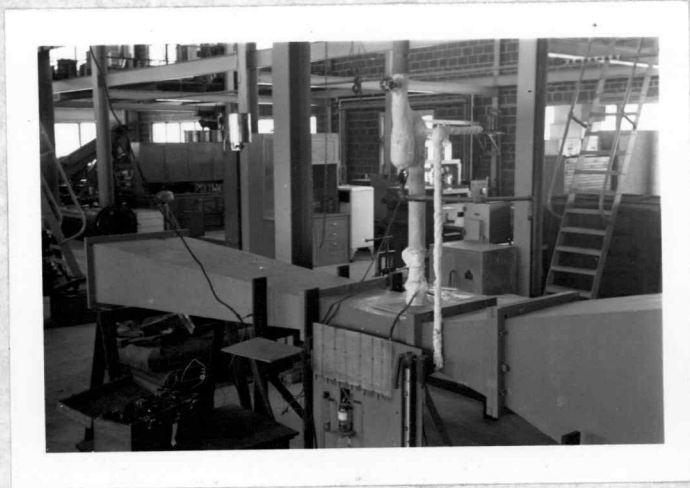


WIND TUNNEL

FIGURE 7



View of wind tunnel looking upstream
from working section.



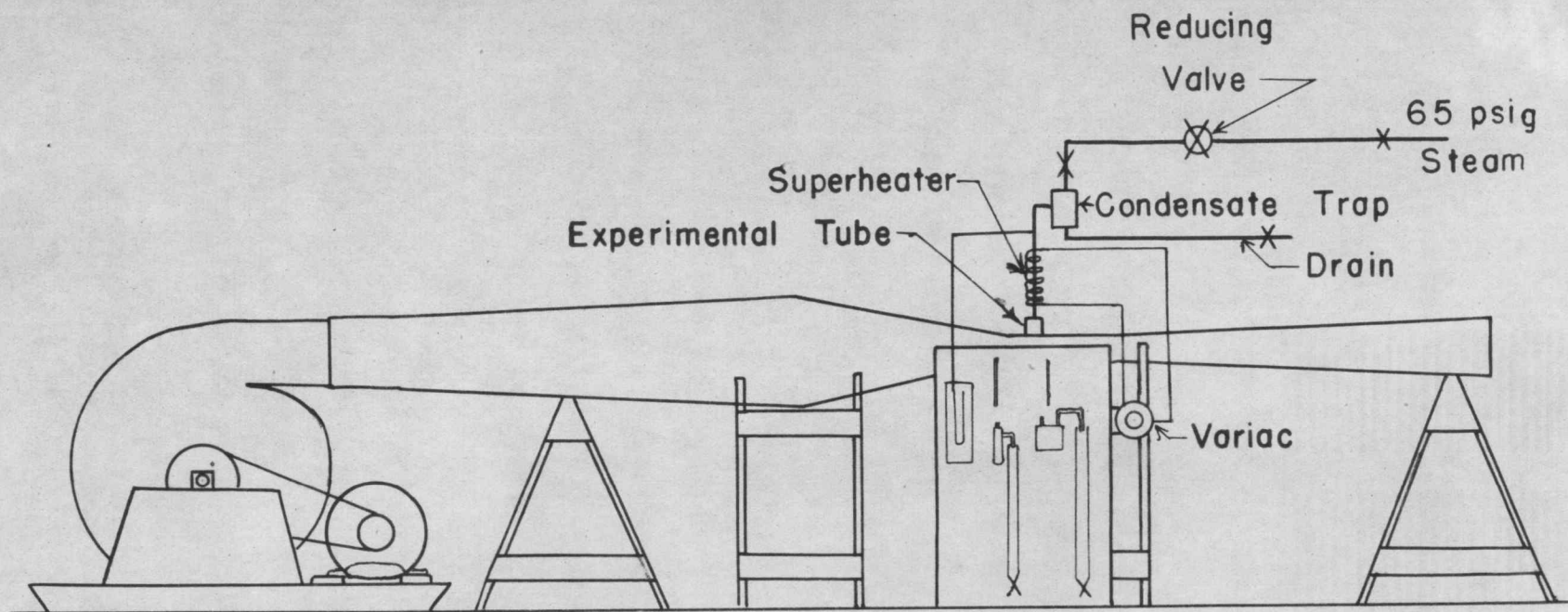
View of wind tunnel looking downstream
from accelerating section.



Side View of tunnel showing parts of the initial and final expansion sections, acceleration section, and working section.



View of instrument board. Shows steam pressure manometer, mercury traps, condensate level indicators, variac, potentiometer.



GENERAL EQUIPMENT LAYOUT

FIGURE 8

A four-inch length was indexed into ten equal sections around the internal periphery and grooved by hand shaping to receive $1/16"$ x $1/4"$ x $4"$ fins. Unfortunately the indexing and shaping were not both done on the same lathe, with the result that all sectors were not exactly equal. Copper fins were fitted into the slots and brazed in with Sil-Fos. A brass ring three-eighths of an inch high was machined to fit snugly against fin edges and brazed to the bottom three-eighths inches of each fin so as to form a dam for each sector, thus the bottom of the dam was level with the bottom of the experimental section. Lengths of three-eighths inch copper tubing were then brazed in at the bottom of each sector to serve as condensate drains. These were brought down through a bottom guard section of the two-inch copper pipe and extended outside for two inches.

The bottom guard section was a nine-inch piece of the two-inch copper pipe brazed to the bottom of the experimental section. While making a run, saturated steam was circulated in it to prevent condensate from forming in the collection tubes. Directly above the experimental section was brazed a five-inch length of the copper pipe fitted with a $1/16"$ plate at the floor having a one-inch hole

surrounded by a copper dam one-half inch in height which served as a steam chest and top guard section. A $1" \times 1\frac{1}{4}"$ plate was placed above the one-inch hole to prevent condensate from dripping into the experimental section. Steam entered the chest from above and then passed into the experimental section through the one-inch opening. Condensate from the walls of the steam chest was drained from the chest floor by a $3/16"$ copper tube leading past the experimental section into the bottom guard section. The $1/8"$ vents were brought out from above two diametrically opposed fins of the experimental section. There was also a combination vent-drain from the bottom guard section.

The top of the steam chest was covered with a copper plate to which a $3/4"$ cross was brazed. One end of the cross was connected to the steam supply, a thermometer was placed in the path of the entering steam through another, and the third was plugged. Construction details are shown in Figures 9 and 10.

Constantan wire was soldered in "fins" number 3 and 7 and a common copper wire attached at the top of the tube for obtaining the temperature of the condensing steam. The term "fin" as used here refers to the sector between two actual fins. This meaning will be continued henceforth.

CROSECTION OF EXPERIMENTAL TUBE

25

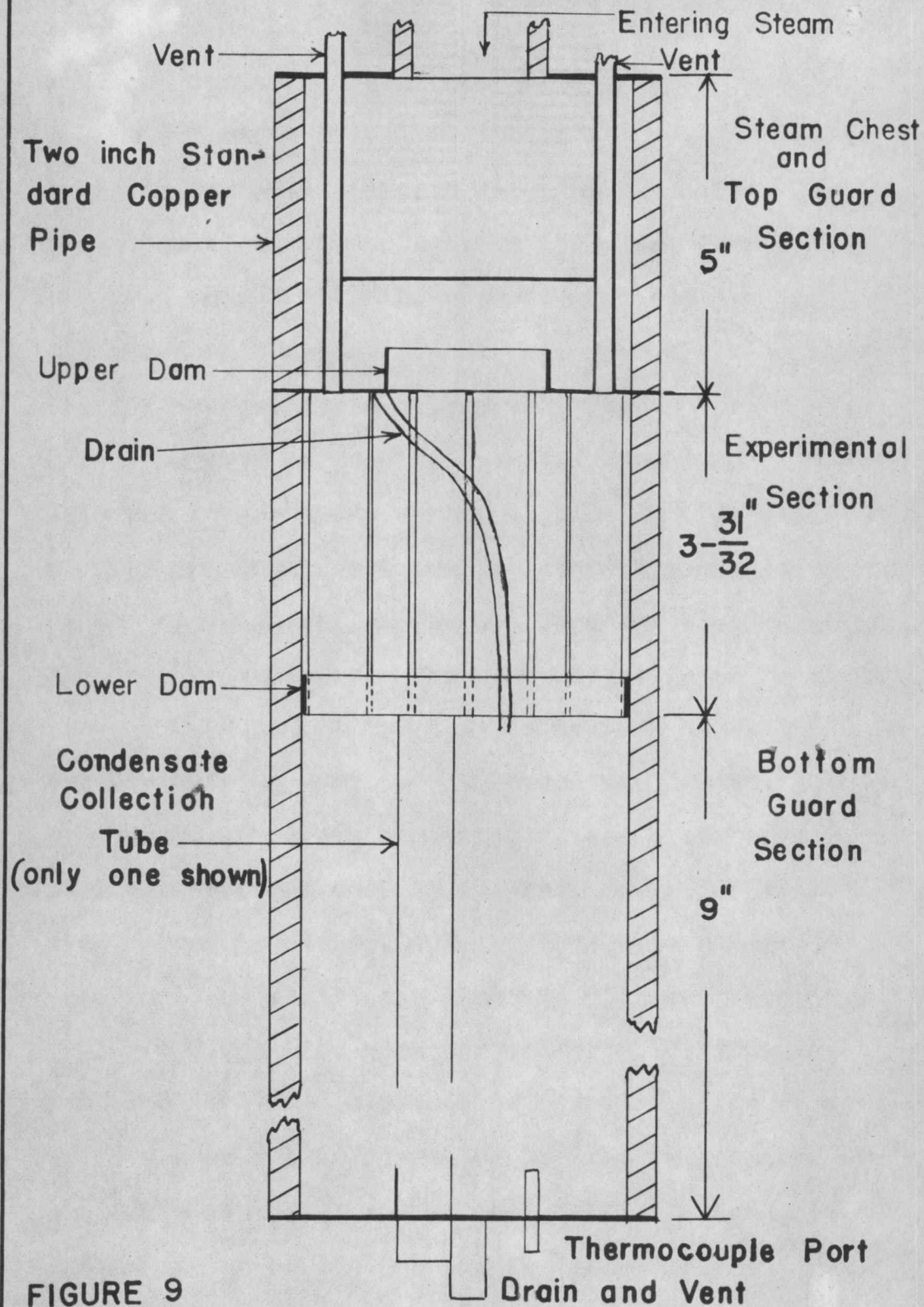


FIGURE 9

TOP VIEW OF EXPERIMENTAL
SECTION: GUARD SECTIONS
REMOVED

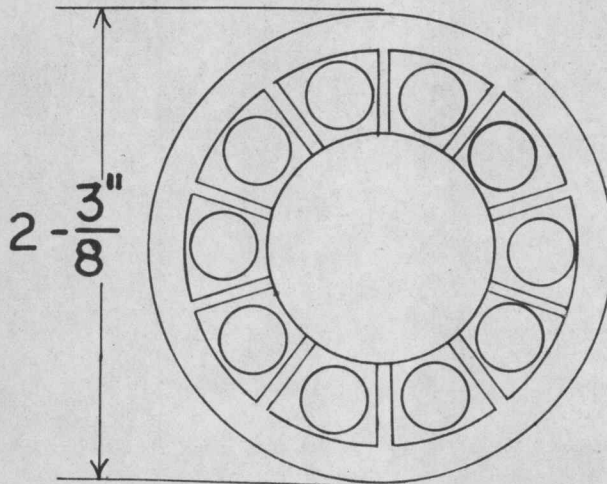


FIGURE 10

Steam was reduced from 65 psig to about 0.5 inches of water gage, passed through a water trap, and then superheated to approximately 218°F . with a variac controlled electric heater just before entering the experimental tube.

The tube was mounted in the working section so it could be readily rotated. It was supported by a clamp bearing on the top of the tunnel. The tube was located ten inches downstream in the working section, and the four inch experimental section was centered in the 6" x 18" tunnel section.

The condensate was drained from the experimental section through the bottom guard section to a mercury non-return trap from which it was collected in a burette. A glass tee was placed ahead of the mercury trap from which a stand pipe was brought out to indicate the liquid level in the sump (guard section). All connections were made with Tygon tubing. This allowed visual inspection if air was trapped in the lines. Sufficient play was left to allow the tube to be rotated about 90° without changing connections.

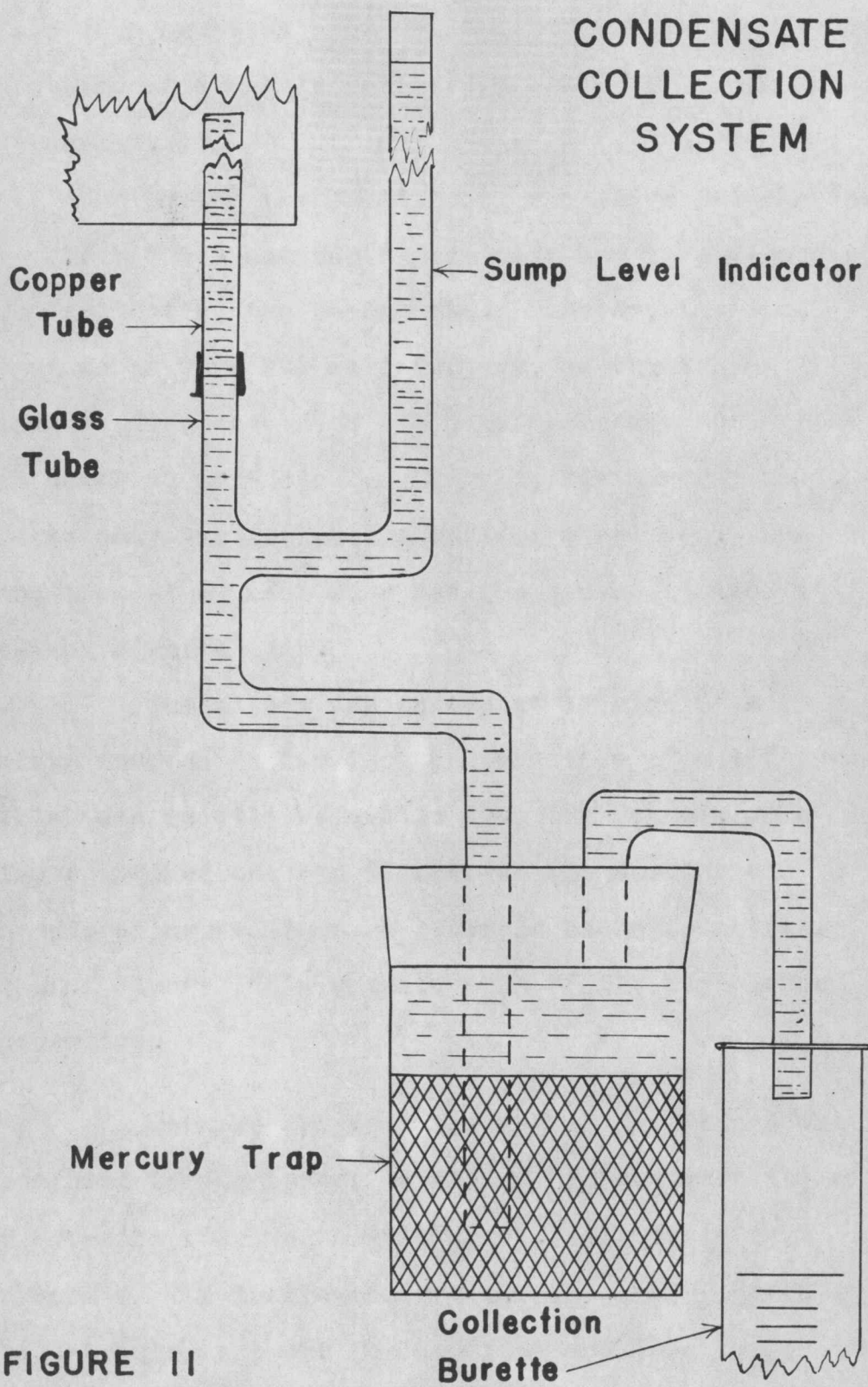
The mercury trap served a two-fold purpose. First, it kept the liquid level up in the sump while actual collection took place below it, and, second, it prevented air from being drawn into the system in

case of a negative pressure change in the steam supply. A sketch of a single collection system is shown in Figure 11.

During the preliminary runs five 6-inch side arm test tubes and one 8-inch side arm tube were used for collecting the condensate. However, the small test tubes were not satisfactory, as the amount of mercury displaced from the water tube was sufficient to cause an appreciable change in the mercury head. Later only two collection systems were used. One was the 8-inch test tube and the other utilized a 3-inch diameter jar.

Turbulence was generated by nine $\frac{1}{2}$ " x 1" x 6" slats mounted on two inch centers in a 6" x 18" frame which was readily removable from the tunnel. The frame matched the end flanges of the working and accelerating sections so it could be bolted between them. Figure 12 is a photograph of the turbulence generator.

Measurement of Turbulence: Turbulence was measured in the manner developed by Schubauer (8) with a hot-wire wake angle instrument. Figure 13 is a sketch of the instrument probe. This was mounted in a ball bearing support for mounting and rotating in the tunnel. Figure 14 is a photograph of the assembled

**FIGURE II**

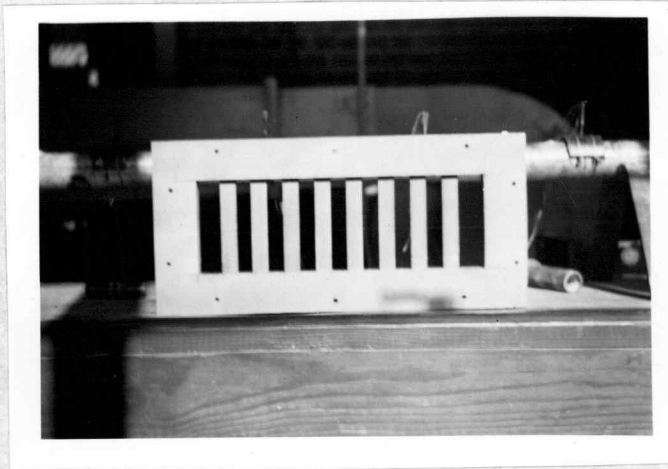


FIGURE 12 TURBULENCE GENERATOR

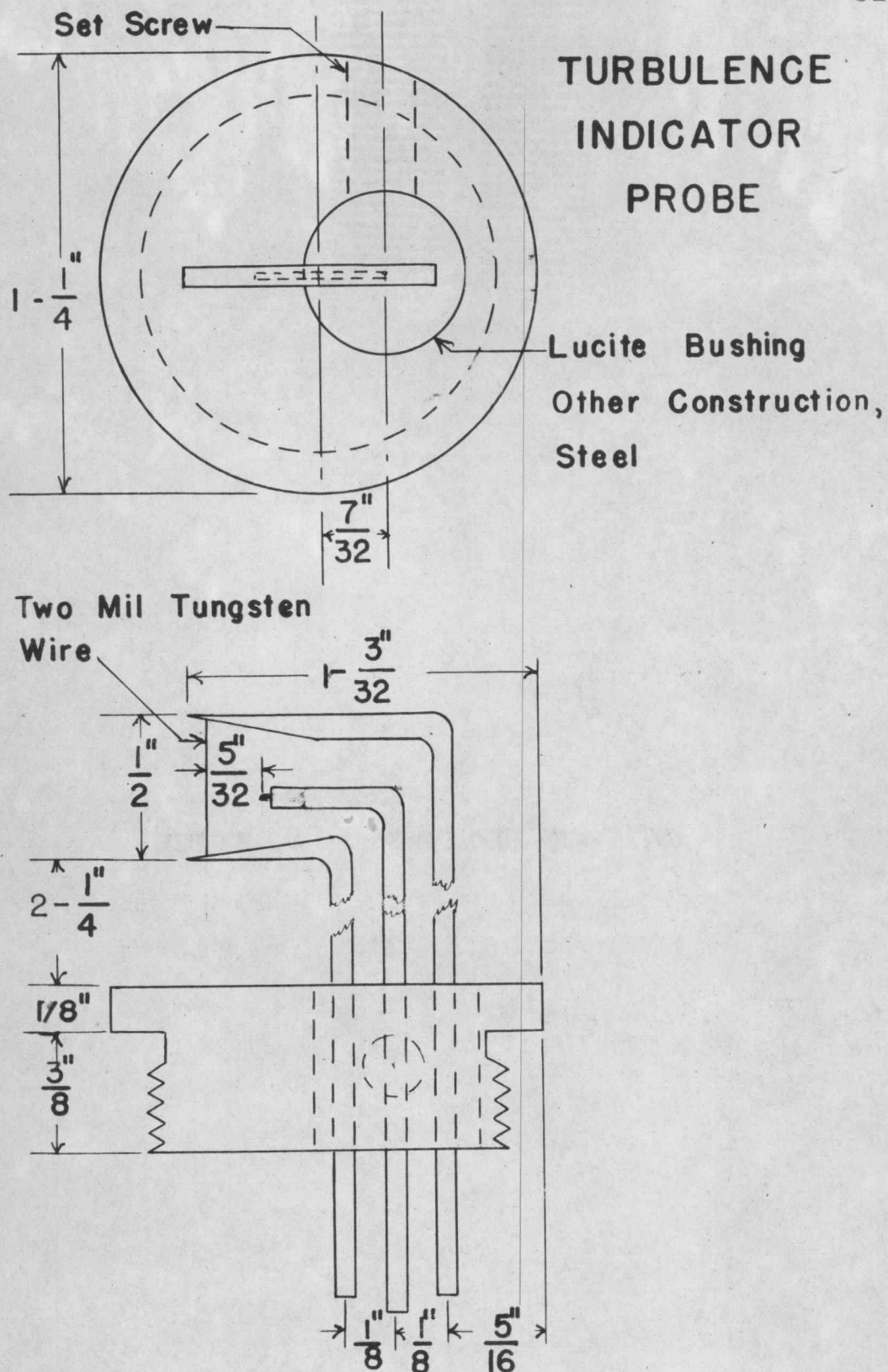


FIGURE 13

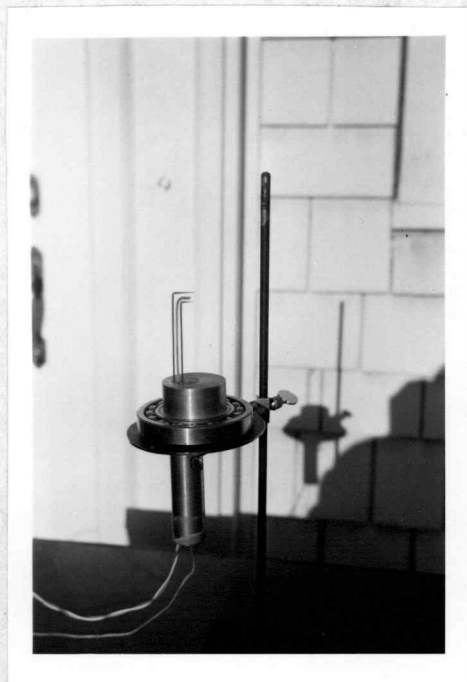


FIGURE 14 TURBULENCE MEASURING
INSTRUMENT

instrument.

It has been found that with increasing turbulence the width of the heated wake of a hot wire increases, indicating a relation between the rate of diffusion and the degree of turbulence of the air stream.

For laminar, uniform, flow, assuming the heated wire's diameter is so small as to be negligible, the temperature distribution at points not too close to the wire* is given by the equation,

$$\Delta T = \Delta T_{\max} e^{\frac{-y^2 \rho c v}{4kx}} \dots\dots\dots(6)$$

where:

- y = distance across wake measured from center
- x = distance downstream from wire
- ΔT = temperature rise at any point
- ΔT_{\max} = maximum temperature rise at the point (x,0)
- v = air speed
- ρ = density of air
- c = specific heat of air at constant pressure
- k = thermal conductivity of air

The finite size of the wire, the conduction of heat in the x direction and the effect of the wire on flow in

*That is, the quantity $\frac{\rho c v}{2k} \sqrt{x^2 + y^2}$ is large.

the wake have been neglected.

If the stream is turbulent, there is an apparent conductivity, $(k + B)$ where B is the eddy conductivity due to the turbulence. Hence the above equation becomes:

$$\Delta T = \Delta T_{\max} e^{-\frac{y^2 \rho c v}{4(k+B)x}} \dots\dots\dots(7)$$

The width of the heated wake at half the maximum temperature change is selected to represent the width characteristic of the wake. Hence:

$$\frac{\Delta T}{\Delta T_{\max}} = \frac{1}{2} = e^{-\frac{y^2 \rho c v}{4kx}} \dots\dots\dots(8)$$

where y represents the half width, and $2y$ then represents the width characteristic. Changing to angular measure and solving for α_0 , the total angle subtended at the wire by the wake width at $\frac{\Delta T}{\Delta T_{\max}} = \frac{1}{2}$ for laminar flow:

$$\alpha_0 = 190.8 \sqrt{\frac{k}{\rho c v x}} \dots\dots\dots(9)$$

Similarly, for turbulent flow:

$$\alpha = 190.8 \sqrt{\frac{(k+B)}{\rho c v x}} \dots\dots\dots(10)$$

where α is the angular width for turbulent flow.

Then,

$$\alpha^2 = \frac{36,400 k}{\rho c v x} + \frac{36,400 B}{\rho c v x} = \alpha_0^2 + \alpha_t^2 \dots\dots\dots(11)$$

where α_t is the angular width due to turbulence alone.

Hence:

$$\alpha_t^2 = \alpha^2 - \alpha_o^2 \dots\dots\dots(12)$$

Since the turbulence level Z is proportional to α_t :

$$Z = c \alpha_t$$

The constant, c, was found by Schubauer (8 p.4) to

equal $\frac{1}{1.53}$, Therefore:

$$Z = \frac{\alpha_t}{1.53} \dots\dots\dots(13)$$

It should be noted that this instrument does not completely characterize the turbulence. It measures the intensity, but not the scale, or eddy size, of the turbulence.

Procedure: Originally it was planned to collect condensate individually from five consecutive fins, subtending a total angle of 180° to the direction of flow. The other five fins should, by the symmetry of the equipment, produce equivalent results. The condensate from these fins was to be measured collectively as a check on the other half of the tube. However, the initial runs indicated that the presence of leaks or other disturbing factors were influencing the results of some particular fins. Therefore, two adjacent fins which gave apparently reliable and consistent results were used for the final

experimental runs.

A run was conducted in the following manner: The tube was rotated to the desired position and the blower and steam turned on. All condensate lines were then well bled with steam and allowed to fill with condensate. Air velocity was measured thirteen inches upstream from the experimental section with an Alnor velometer and the damper on the blower inlet adjusted to give the desired flow. The steam pressure was regulated at about 0.5 inch of water gage and the variac adjusted to give a steam temperature of about 218°F. The condensate collection rate was then allowed to reach equilibrium. Burette and level indicator readings were taken every minute, i.e. when collection was being made from the five individual and one collective fins, each burette was read once every six minutes. However, when only two burettes were being used, each was read once every two minutes except at low condensation rates (less than 0.7cc. per minute) when readings were sometimes taken only once every two minutes, i.e. each burette was read once every four minutes. Readings were continued until at least 20 cc. had been collected with no individual reading deviating more than 2% from the total collected, or 10 cc. with no individual reading deviating more than

1% from the total collected. The smaller quantity was collected when the condensation rate was so slow that time became important. (Steam was available only for about nine hours, thus limiting the time available for a complete traverse of the tube.) The tube was then rotated one position, allowed to reach equilibrium, and the process repeated. Other measurements periodically observed were: air temperature 13 inches upstream from the working section, barometric pressure, relative humidity, air velocity 13 inches upstream from the working section, blower RPM, static pressure in the tunnel 3 feet upstream from the working section, and steam pressure and temperature.

Turbulence level measurements were made at the same point as the center line of the tube after the experimental runs by removing the experimental tube and inserting the hot wire instrument at the top of the tunnel. The instrument was rotated by hand, and the galvanometer deflections at various angles were noted. From these data the turbulence level was determined.

Calculations: The heat transfer results were calculated as Nusselt numbers for correlation with the Reynolds numbers and the turbulence levels. The local

coefficients were calculated assuming the heat loss due to radiation was negligible and that no heat flowed around the periphery of the tube. These assumptions are justifiable when the accuracy of the results, probably no greater than 10%, is considered.

$$\text{Then: } Nu = \frac{h D_o}{k_f}$$

$$h = \frac{q}{A \Delta t}$$

$$q = (60)(2.4) * R_c = 128.4 R_c, \text{ Btu/hr.}$$

where R_c = condensation rate, cc./minute. Hence:

$$Nu = \frac{q D_o}{k_f A t} = \frac{128.4 R_c D_o}{k_f A \Delta t}$$

$$D_o = \frac{2.375}{12} = 0.198 \text{ ft.}$$

$$Nu = \frac{25.4 R_c}{k_f A \Delta t} \dots\dots\dots(14)$$

It must be remembered that h is actually based on the total driving force from the condensing steam to the ambient air. All units are on the pound, hour, foot, degree Fahrenheit basis.

The outside area was chosen as the basis for the calculations. The area of fin number one was 0.02150 square feet and that of number two 0.02020 square feet, hence the area could not be incorporated into the constant. The temperature at which k_f was obtained was taken as the

* 2.4 Btu/cc = Heat of cond. of steam at 212°F.

arithmetical mean of the air temperature and the tube wall temperature.

A sample calculation is as follows:

$$\begin{array}{lll} \text{run \#40} & t_a = 80 & \Delta t = 212 - 80 = 132^\circ\text{F} \\ \text{fin \#1A} & t_f = 146 & R_e = 0.950 \text{ cc/min.} \\ A = 0.0215 & k_f = 0.01662 & \end{array}$$

$$N_u = \frac{(25.4)(0.50)}{(0.01662)(0.0215)(132)} = 508$$

The Reynolds number was based on the outside diameter of the experimental tube and the velocity in the unobstructed working section. The density and viscosity of air at 75°F . were used for all cases, hence,

$$R_e = \frac{D V \rho}{\mu}$$

$$\rho = 7.4 \times 10^{-2} \text{ lbs/ft}^3$$

$$\mu = 1.19 \times 10^{-5} \text{ lbs/sec-ft.}$$

$$R_e = \frac{(0.198)(7.4 \times 10^{-2})V}{1.19 \times 10^{-5}} = 1,232 V \quad \dots(15)$$

$$V = \text{velocity, ft/second}$$

The turbulence level was obtained from the angular width of a thermal wake behind a hot wire in the manner indicated in the discussion on the measurement of turbulence.

The angular width of the wake at one-half the

maximum galvanometer deflection was read from a plot of the experimental data, Figures 21 through 23. This angle was converted to percent turbulence by the following expression:

$$Z = \frac{\sqrt{\alpha^2 - \alpha_0^2}}{1.53}$$

$$\alpha_0 = 190.8 \sqrt{\frac{k}{\rho c v x}}$$

Sample Calculation:

$$k = 0.01495$$

$$v = 1400 \text{ fpm}$$

$$\rho = 7.4 \times 10^{-2}$$

$$c_p = 0.24$$

$$x = 0.013$$

$$\alpha = 6.5^\circ$$

$$\alpha_0 = 190.8 \sqrt{\frac{(0.01495)(60)}{(7.4 \times 10^{-2})(0.240)(1400)(0.013)}}$$

$$= 5.3^\circ$$

$$Z = \frac{[(6.5)^2 - (5.3)^2]^{\frac{1}{2}}}{1.53} = \frac{\sqrt{14.1}}{1.53} = 2.6\%$$

RESULTS AND DISCUSSION

Four conditions were studied: (1) high velocity with high turbulence, (2) high velocity with low turbulence, (3) low velocity with high turbulence, and (4) low velocity with low turbulence. The high velocity was 86.5 feet per second and the low velocity 28.8 feet per second, giving Reynolds numbers of 106,800 and 35,500 respectively. The high turbulence level was 27%, and the low was 2.6%.

Table I presents the original experimental data of the final runs.* Table II is a tabulation of the calculated results. Individual fin results are plotted in polar coordinates in Figures 15 through 18. Figure 19 is a rectangular coordinate plot of the local heat transfer coefficients for each of the four conditions.

The effect of increasing the turbulence and/or the Reynolds number on the average Nusselt number compares favorably with the extrapolated curve of Comings et al (3 p.1079) as shown by Figure 20.

The variation in the results of two fins for the same position was as great as 15% from the mean

* The data of numerous preliminary runs made to determine final operating techniques are not included.

EXPERIMENTAL DATA

TABLE I

Run No.	Angular Location Degrees From Front of Tube	Fin No.	Velocity	Turb. Level	Temp. Air °F	Rate of Condensation c.c./min.
30	324-360	2	86.5	27%	80	1.042
30	0-36	1	86.5	27%	80	0.950
30	0-36	2	86.5	27%	80	0.998
30	36-72	1	86.5	27%	80	0.854
31	0-36	2	86.5	27%	76	1.018
31	36-72	1	86.5	27%	76	0.882
31	36-72	2	86.5	27%	77	0.933
31	72-108	1	86.5	27%	77	0.768
31	72-108	2	86.5	27%	77	0.823
31	108-144	1	86.5	27%	77	0.650
31	108-144	2	86.5	27%	78.5	0.721
31	144-180	1	86.5	27%	78.5	0.566
31	144-180	2	86.5	27%	79	0.653
31	180-216	1	86.5	27%	79	0.558
32	144-180	2	86.5	27%	76	0.703
32	180-216	1	86.5	27%	76	0.610
32	180-216	2	86.5	27%	77	0.714
32	216-252	1	86.5	27%	77	0.716
32	216-252	2	86.5	27%	76.5	0.790
32	252-288	1	86.5	27%	76.5	0.805
32	252-288	2	86.5	27%	77	0.899
32	288-324	1	86.5	27%	77	0.938
32	288-324	2	86.5	27%	77	1.030
32	324-360	1	86.5	27%	77	1.038
32	324-360	2	86.5	27%	77	1.104
32	0-36	1	86.5	27%	77	1.021
32	0-36	2	86.5	27%	77	1.054
32	36-72	1	86.5	27%	77	0.888
32	36-72	2	86.5	27%	76.5	0.948
32	72-108	1	86.5	27%	76.5	0.741
33	72-108	2	86.5	27%	72	0.865
33	108-144	1	86.5	27%	72	0.690
33	108-144	2	86.5	27%	74.5	0.766

TABLE I (continued)

Run No.	Angular Location Degrees From Front of Tube	Fin No.	Velocity	Turb. Level	Temp. Air °F	Rate of Condensation c.c./min.
33	144-180	1	86.5	27%	74.5	0.562
33	144-180	2	86.5	27%	76.5	0.685
33	180-216	1	86.5	27%	76.5	0.560
34	324-360	2	28.8	27%	81	0.530
34	0-36	2	28.8	27%	81	0.486
34	0-36	1	28.8	27%	79.5	0.515
34	36-72	2	28.8	27%	79.5	0.429
34	36-72	1	28.8	27%	79	0.452
34	72-108	2	28.8	27%	79	0.333
35	72-72	2	28.8	27%	76.5	0.461
35	72-108	1	28.8	27%	77.5	0.372
35	72-108	2	28.8	27%	77	0.404
35	108-144	1	28.8	27%	77	0.300
36	72-108	2	28.8	27%	78.5	0.340
36	108-144	1	28.8	27%	78.5	0.327
36	108-144	2	28.8	27%	79	0.314
36	144-180	1	28.8	27%	79	0.297
36	144-180	2	28.8	27%	79	0.299
36	180-216	1	28.8	27%	79	0.285
37	324-360	2	86.5	2.6%	72	0.805
37	0-36	1	86.5	2.6%	72	0.683
37	0-36	2	86.5	2.6%	75	0.698
37	36-72	1	86.5	2.6%	75	0.570
37	36-72	2	86.5	2.6%	74.5	0.683
37	72-108	1	86.5	2.6%	74.5	0.525
37	72-108	2	86.5	2.6%	75	0.680
37	108-144	1	86.5	2.6%	75	0.596
37	108-144	2	86.5	2.6%	76.5	0.786
37	144-180	1	86.5	2.6%	76.5	0.716
37	144-180	2	86.5	2.6%	76.5	0.913
37	180-216	1	86.5	2.6%	76.5	0.734
37	180-216	2	86.5	2.6%	76	0.840
37	216-252	1	86.5	2.6%	76	0.601
37	216-252	2	86.5	2.6%	76	0.683
37	252-288	1	86.5	2.5%	76	0.495
37	252-288	2	86.5	2.6%	78	0.544
37	288-324	1	86.5	2.6%	78	0.531

TABLE I (continued)

Run No,	Angular Location Degrees From Front of Tube	Fin No.	Velocity	Turb. Level	Temp. Air °F	Rate of Condensation c.c./min.
38	324-360	2	28.5	2.6%	75	0.384
38	0-36	1	28.5	2.6%	75	0.393
38	0-36	2	28.5	2.6%	76.5	0.413
38	36-72	1	28.5	2.6%	76.5	0.260
38	36-72	2	28.5	2.6%	76.5	0.278
38	72-108	1	28.5	2.6%	76.5	0.212
38	72-108	2	28.5	2.6%	76.5	0.249
38	108-144	1	28.5	2.6%	76.5	0.232
38	108-144	2	28.5	2.6%	77	0.338
38	144-180	1	28.5	2.6%	77	0.310
38	144-180	2	28.5	2.6%	77	0.418
38	180-216	1	28.5	2.6%	77	0.300

CALCULATED RESULTS

TABLE II

Run No.	Reynolds Number	Turb. Level	Fin No.	Local Nusselt Number										Average Nusselt Number
				18°	54°	90°	*Degrees From Front of Tube				270°	306°	342°	
							126°	162°	198	234				
30	106,800	27%	1	508	459									600
30	106,800	27%	2	575										
31	106,800	27%	1		462	405	342	302	299					
31	106,800	27%	2	567	526	463	412	372						
32	106,800	27%	1	536	469	388			319	376	424	495	547	
32	106,800	27%	2		532			394	402	443	505	605	624	
33	106,800	27%	1				350	289	294					
33	106,800	27%	2			470	423	384						268
Average values runs 30-33:														
			1	522	464	396	345	296	304	376	424	496	546	418
			2	580	530	466	417	384	402	443	505	606	624	495
	Avg.		1 and 2	551	497	431	381	340	353	409	464	551	585	456
34	35,500	27%	1	263	230	174								
34	35,500	27%	2	296	259									307
35	35,500	27%	1			196	158							
35	35,500	27%	2		258	227								
36	35,500	27%	1				174	158	153					
36	35,500	27%	2			194	180	171						
Average values runs 34-36:														
			1	263	230	185	166	158	153					201
			2	296	258	211	180	171					307	221
	Avg.		1 and 2	279	244	198	173	165	153				307	211

CALCULATED RESULTS
TABLE II (continued)

Run No.	Reynolds Number	Turb. Level	Fin No.	Local Nusselt Number										Average Nusselt Number
				18°	54°	90°	*Degrees 126°	From 162°	Front 198°	of 234°	Tube 270°	306°	342°	
37	106,800	2.6%	1	346	295	272	308	376	384	313	259	282		318
37	106,800	2.6%	2	386	377	378	441	511	469	380	308		435	403
Average			1 and 2	366	336	325	374	443	426	347	384	282	435	360
38	35,500	2.6%	1	204	136	111	119	163	158					147
38	35,500	2.6%	2	232	156	140	186	235					219	190
Average			1 and 2	218	146	126	152	199	158				219	168

HEAT TRANSFER COEFFICIENT DISTRIBUTION

 $Re = 106800$

27% Turbulence

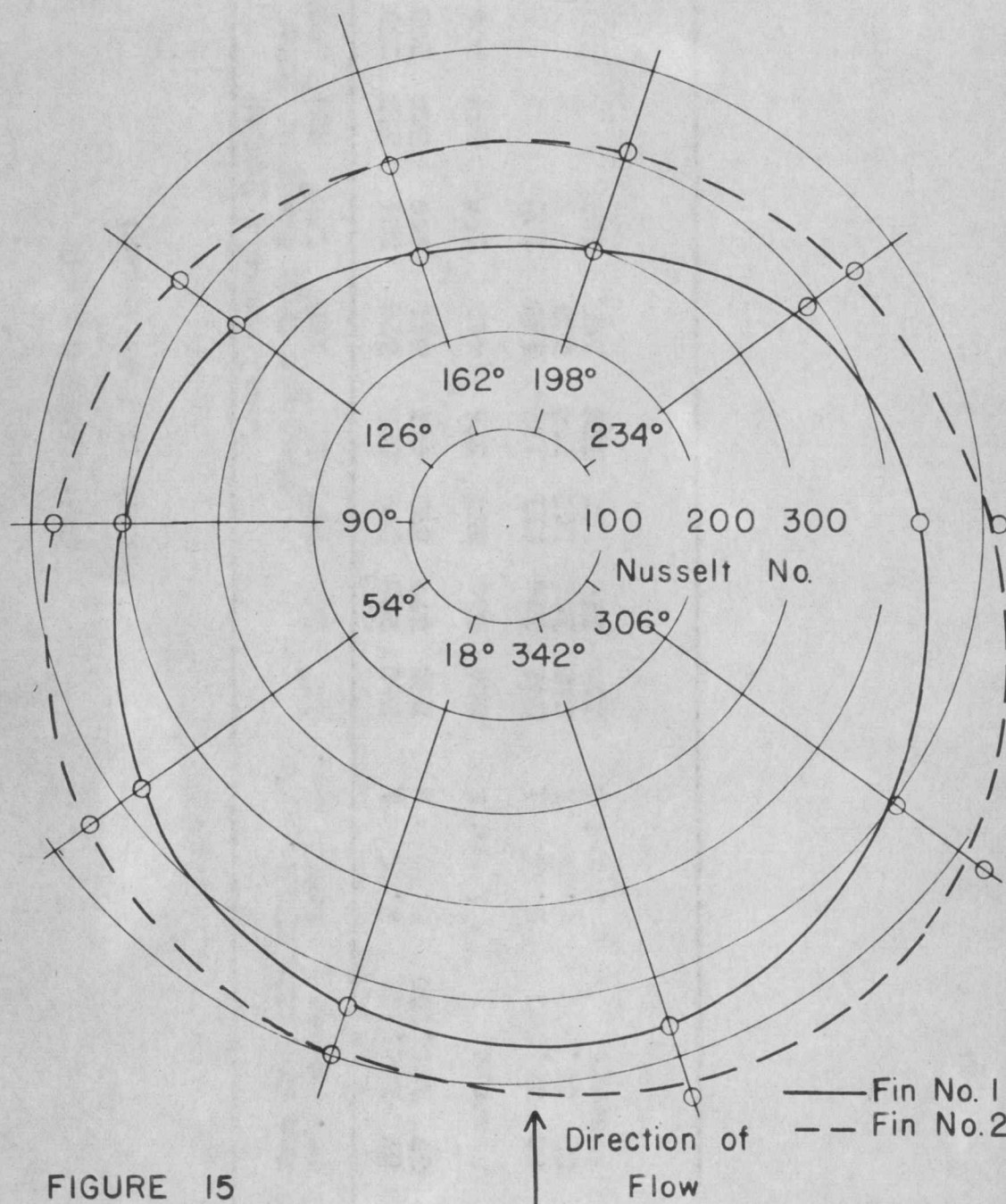
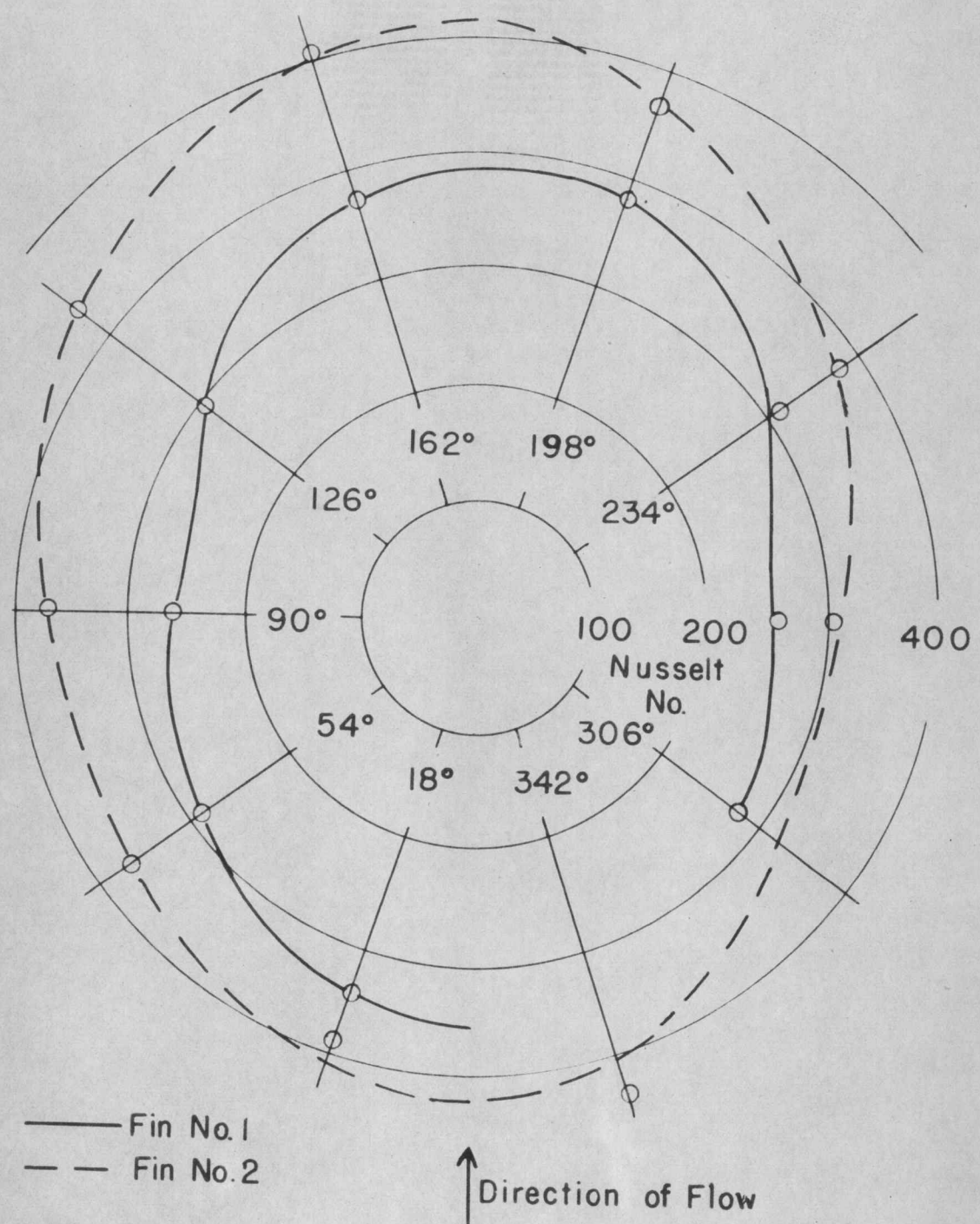


FIGURE 15

Re= 106800

2.6% Turbulence

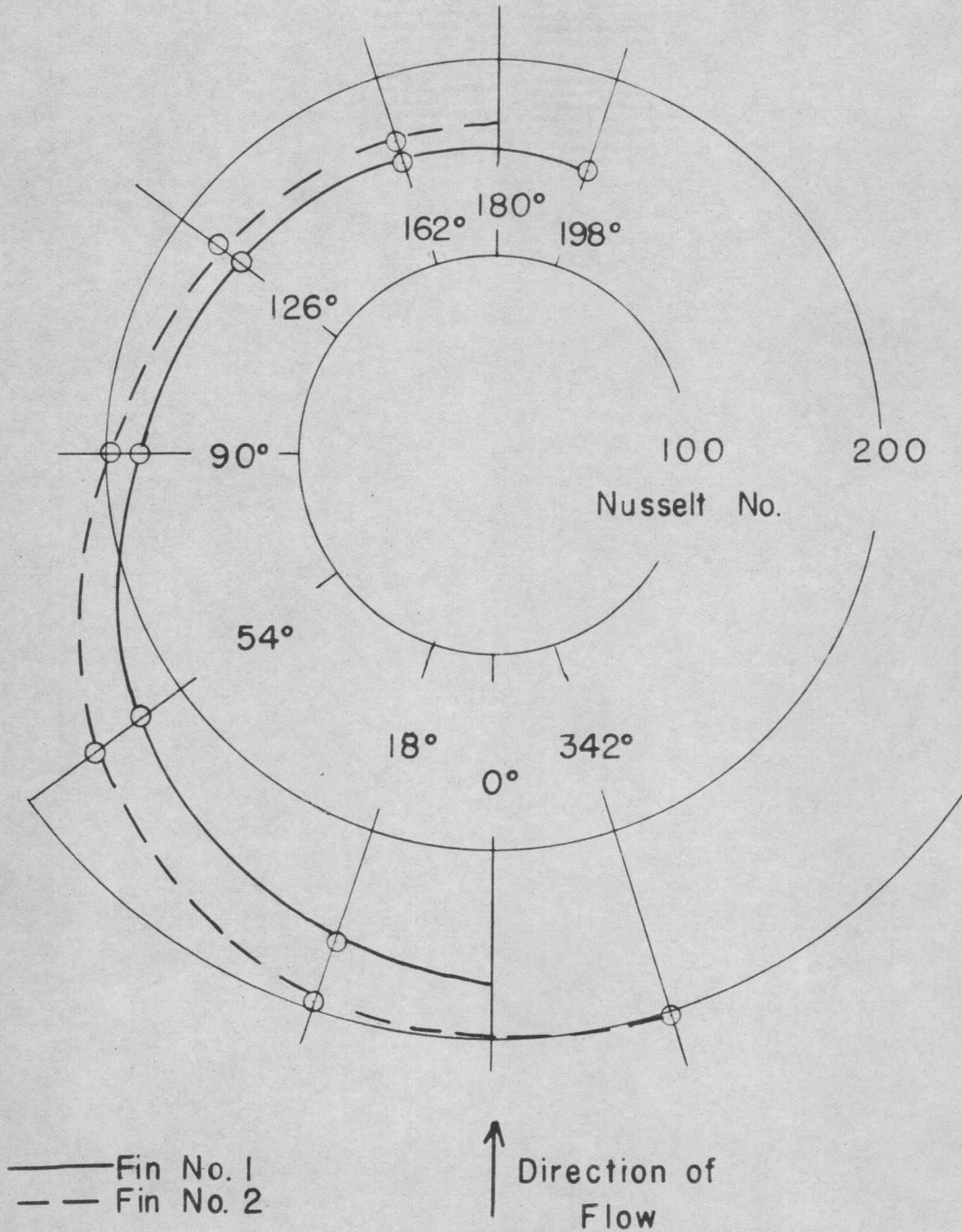


HEAT TRANSFER COEFFICIENT DISTRIBUTION

FIGURE 16

$Re = 35500$

27% Turbulence



HEAT TRANSFER COEFFICIENT DISTRIBUTION

FIGURE 17

HEAT TRANSFER COEFFICIENT DISTRIBUTION

 $Re = 35500$

2.6% Turbulence

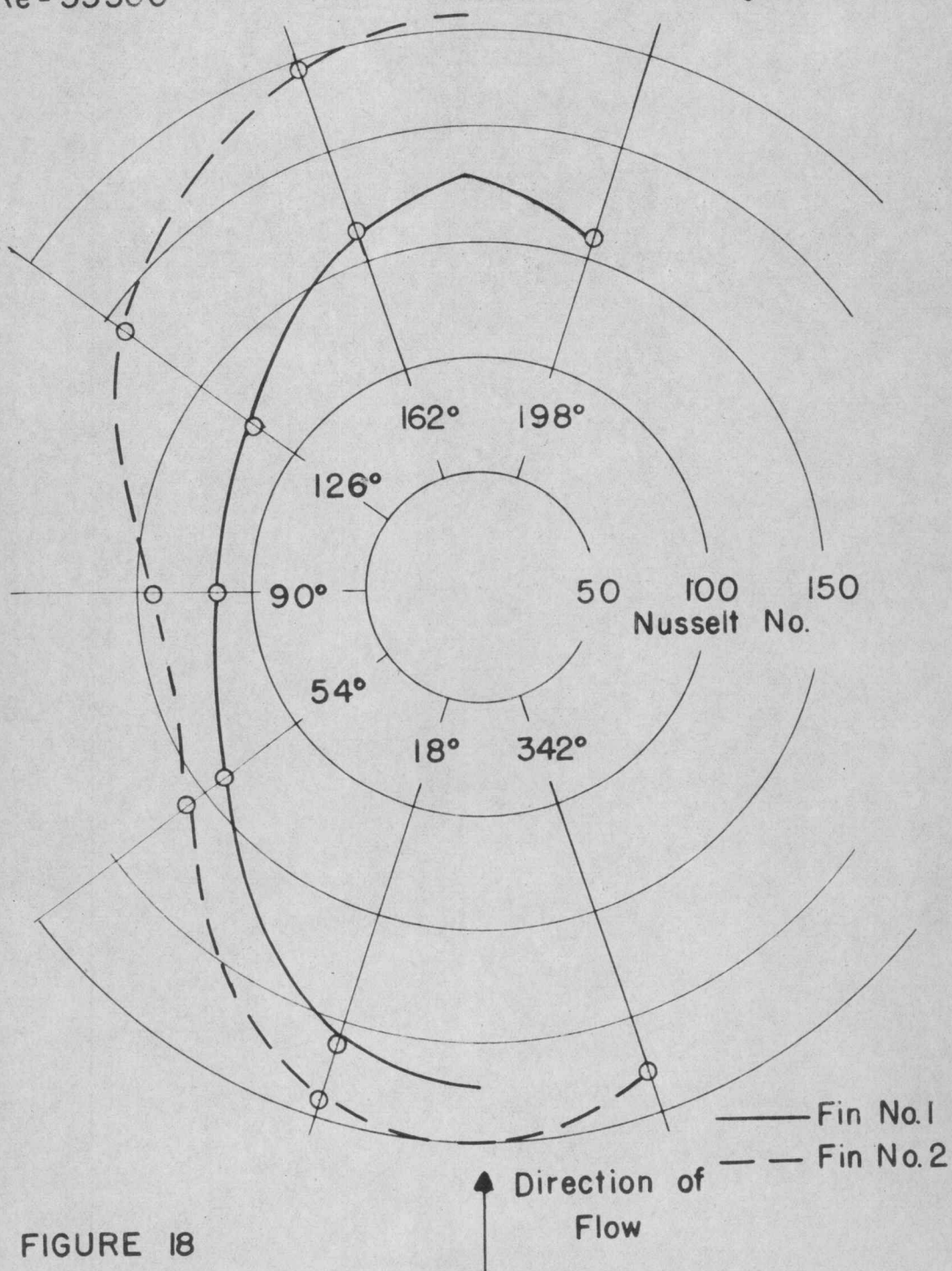


FIGURE 18

HEAT TRANSFER COEFFICIENT DISTRIBUTIONS

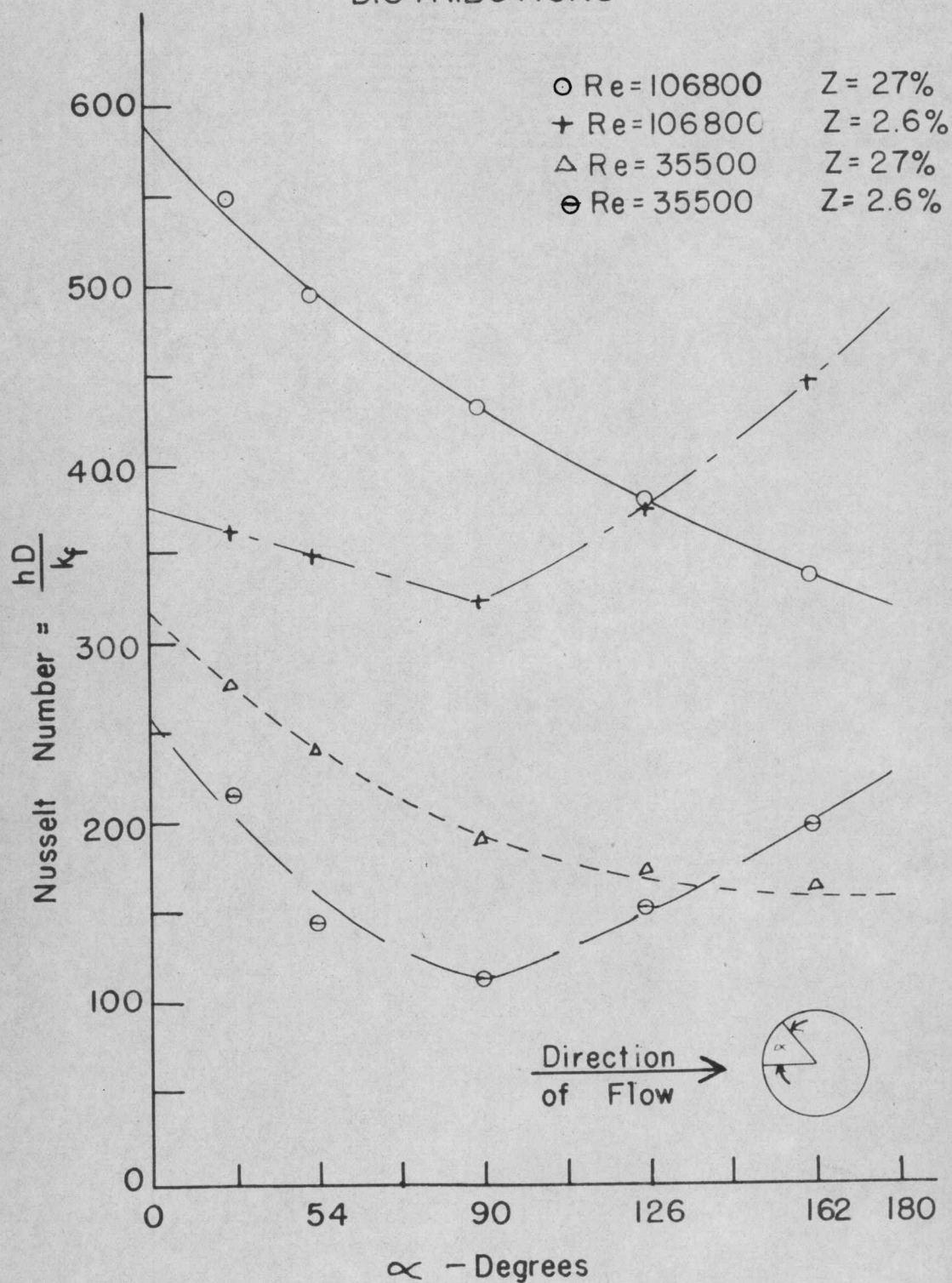
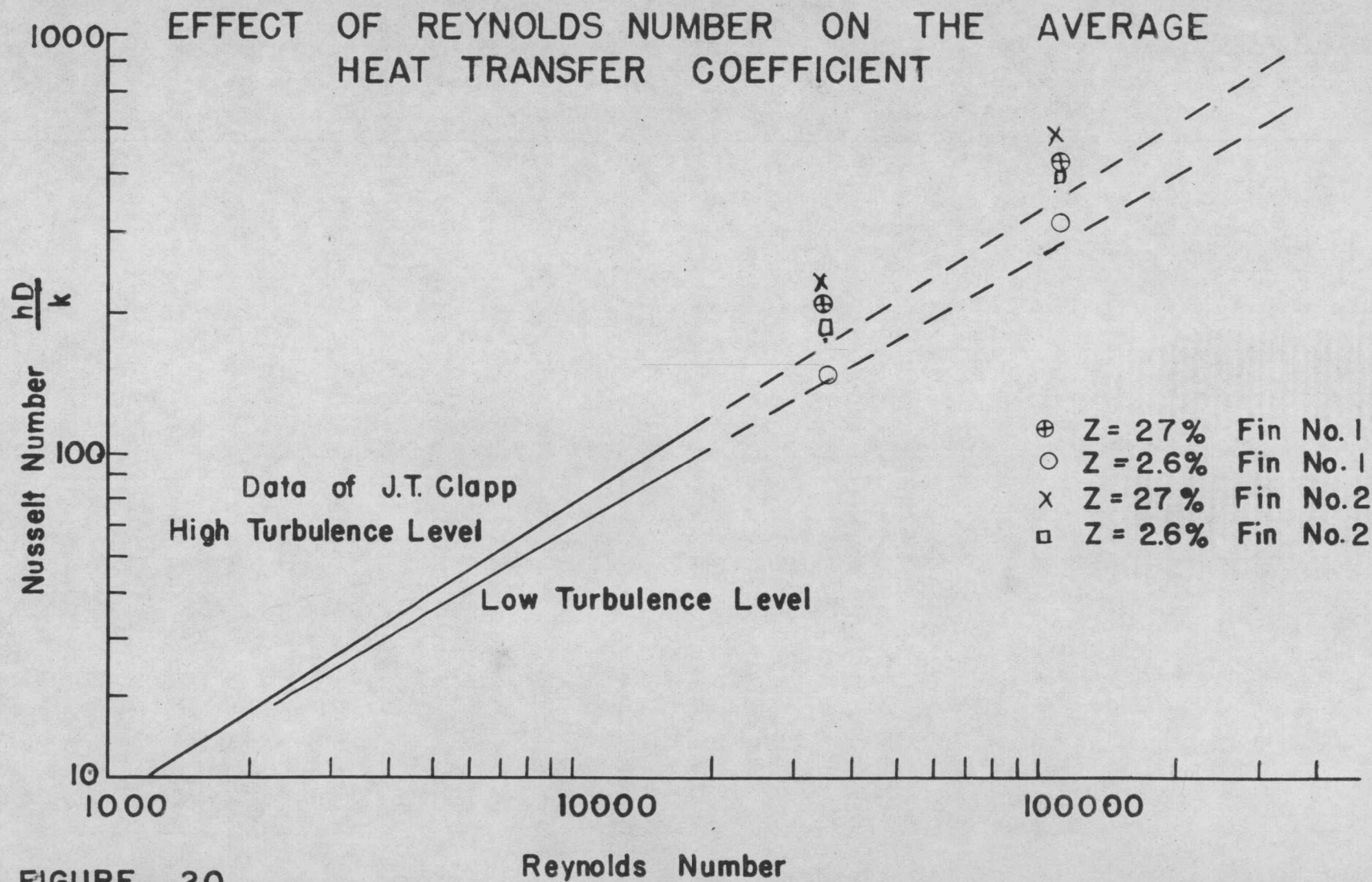


FIGURE 19



of the two. In order to show whether this variation was the result of an error in the fin area measurement, the results were converted to ratios of the Nusselt number for a given fin at any angle to the Nusselt number of that fin at 18 degrees. By this process errors in area cancel out. The ratios thus obtained are shown in Table III. They vary as much as 10% from the mean, indicating some other cause for the discrepancy. With the same fin, results could be reproduced to about 5%.

At low turbulence levels, Figures 15 and 17, the Nusselt number decreases from the front to a minimum at the sides, increasing toward the rear. At the high turbulence levels, Figures 14 and 16, the Nusselt number shows a steady decrease from a maximum at the front to a minimum in the rear. Hence it is seen that abnormally high turbulence levels produce a pronounced change in the normal distribution of the individual heat transfer coefficients.

The behavior at low turbulence levels is readily explained by the boundary layer theory. The increased resistance at the sides is caused by the building up of the boundary layer, and decreased resistance at the rear as the result of turbulent swirls and eddies

COMPARISON OF LOCAL NUSSELT NUMBERS
OF TWO FINS BY RATIOS

TABLE III

Conditions of Run	Re = 106,800 Turb.level = 2.6%		Re = 106,800 Turb.level = 27%		Re = 35,500 Turb.level = 2.6%		Re = 35,500 Turb.level = 27%	
Angle from front of tube	Nu No. @ Angle Nu No. @ 18° Fin #1 Fin #2		Nu No. @ Angle Nu No. @ 18° Fin #1 Fin #2		Nu No. @ Angle Nu No. @ 18° Fin #1 Fin #2		Nu No. @ Angle Nu No. @ 18° Fin #1 Fin #2	
18	1.00	1.00	1.00	1.00	1.00	1.00	1.00	1.00
54	0.85	0.98	0.88	0.91	0.67	0.67	0.88	0.87
90	0.78	0.98	0.76	0.81	0.55	0.60	0.71	0.71
126	0.89	1.14	0.66	0.72	0.59	0.81	0.63	0.61
162	1.08	1.32	0.57	0.66	0.80	1.01	0.60	0.58
198	1.10	1.21	0.58	0.69	0.78		0.58	
234	0.90	0.99	0.72	0.76				
270	0.75	0.80	0.81	0.88				
306	0.81		0.95	1.04				
342		1.13	1.2	1.06		0.94		1.04

formed by separation of the boundary layer.

The high turbulence results are not so readily explicable. The following possible explanations may be put forth: (1) The intensity of turbulence in the stream about the tube is so great that the velocity vectors in all directions are a fairly large fraction of the main stream velocity. (2) The intensity of turbulence of the stream around the tube approaches that produced in the wake of the tube. (3) The turbulent mainstream appears to sweep the boundary layer toward the rear of the tube before separation occurs. No claim is made for any of these hypotheses.

Since the experimental data obtained is too incomplete and not sufficiently reproducible, further experiments with varying intensity of turbulence should be made before definite conclusions can be drawn.

It might be noted that increasing the Reynolds number from 35,500 to 106,800 had little effect on the shape of either distribution curve.

CONCLUSIONS

1. The results show that abnormally high turbulence substantially changes the normal heat transfer coefficient distribution about a cylinder normal to an air stream. The minimum coefficient occurred at the rear of the tube instead of at the side and gradually increased to a maximum at the front.

2. The individual heat transfer coefficient distribution about a tube normal to an air stream flowing at low turbulence was found to be similar to that of previous investigators, i.e. the heat transfer coefficient passed through a minimum at the sides.

3. The average heat transfer coefficient at a Reynolds number of 106,800 was augmented 26% by an increase in the turbulence from 2.6% to 27%. At a Reynolds number of 35,500 there was a 25% increase for a like turbulence change.

4. An increase in the Reynolds number at 2.6% turbulence increased the average Nusselt number from 169 to 457 but did not change the nature of the coefficient distribution. This agrees with previous correlations as does the comparable results at 27% .

turbulence.

APPENDIX

NOMENCLATURE

- A = heat transfer area, sq. ft.
 B = eddy conductivity
 C_p = specific heat, Btu per lb., $^{\circ}\text{F}$
 D = diameter of experimental tube, outside, ft.
 h = local heat transfer coefficient, Btu per hr., sq. ft., $^{\circ}\text{F}$.
 h_s = individual heat transfer coefficient, steam side, Btu per hr., sq. ft., $^{\circ}\text{F}$
 h_b = individual heat transfer coefficient, boundary layer, Btu per hr., sq. ft., $^{\circ}\text{F}$.
 k_f = thermal conductivity, Btu per hr., sq. ft., $^{\circ}\text{F}$ per ft.
 q = rate of heat transfer, Btu per hr. q_r is heat transferred by radiation
 t = temperature, $^{\circ}\text{F}$. t_a = temperature of air, t_s = temperature of steam
 Δt = temperature difference $^{\circ}\text{F}$ between condensing steam in experimental section and air = $t_s - t_a$
 T = temperature, $^{\circ}\text{R}$
 u = local air velocities in direction of flow. u_a = at point a, u_b at point b.
 U = overall heat transfer coefficient, Btu per hr. sq. ft. $^{\circ}\text{F}$

NOMENCLATURE (Continued)

- v = instantaneous velocity vector, \bar{v} = that of basic movement and v' that of the fluctuating velocity. Subscripts x, y, and z refer to direction
- V = velocity of main air stream, ft. per sec.
- x = distance between thermocouple and hot wire, feet
- Z = turbulence level, percent
- Re = Reynolds number = $\frac{DV\rho}{\mu}$
- Nu = Nusselt number = $\frac{hD}{k_f}$
- α = measured angle of turbulence
- α_o = angle due to heat transfer by conduction
- α_t = corrected angle of turbulence
- α_{12} = absorptivity
- ϵ = emissivity
- ρ = density of air, lbs. per cu. ft.
- μ = viscosity of air, lb. per ft. sec.
- ν = kinematic viscosity of air, sq. ft. per sec.

Osborn Reynolds was the first to attempt to describe the nature of turbulence. By considering the instantaneous velocity vector as the vector sum of two different velocities, \bar{v} and v' , the first the time average and the second the fluctuating velocity, and combining with the basic Navier-Stokes equation and the equations of continuity, he obtained the following equation for one coordinate direction:

$$\rho \left[\frac{\partial \bar{v}_x}{\partial t} + \bar{v}_x \frac{\partial \bar{v}_x}{\partial x} + \bar{v}_y \frac{\partial \bar{v}_x}{\partial y} + \bar{v}_z \frac{\partial \bar{v}_x}{\partial z} \right] = - \frac{\partial}{\partial x} (p + \tau_h) + \mu \left[\frac{\partial^2 \bar{v}_x}{\partial x^2} + \frac{\partial^2 \bar{v}_x}{\partial z^2} + \frac{\partial^2 \bar{v}_x}{\partial y^2} \right] - \rho \left[\frac{\partial \bar{v}_x'^2}{\partial x} + \frac{\partial \bar{v}_x' v_y'}{\partial y} + \frac{\partial \bar{v}_x' v_z'}{\partial z} \right]$$

Two similar equations are obtained for the other two coordinate directions.

Note the presence of the terms $\bar{v}_x'^2$, $\bar{v}_x' v_y'$, $\bar{v}_x' v_z'$, which are combined

by Karman to give the coefficient of correlation,

$$\frac{\bar{v}_x' v_y'}{(\bar{v}_x'^2)^{\frac{1}{2}} (\bar{v}_y'^2)^{\frac{1}{2}}}, \text{ previously mentioned.}$$

Prandtl's Mixing Length: In an effort to define the axial velocity component v' transported by cross-current motion, Prandtl introduced his concept

of a mixing length as the cross-current distance a particle could travel when animated by a cross-current impulse. That is, he reasoned that a fluid particle traveling across the flow would cause a fluctuation at its destination proportional to the distance traveled, l , and the mean velocity gradient, hence:

$$v'_x \sim l \frac{dv'_x}{dy} \quad \text{.....(16)}$$

For reasons of continuity,

$$v'_x \sim v'_y \quad \text{.....(17)}$$

and hence the intensity of turbulent shear is:

$$\tau \sim \rho v'_x v'_y \quad \text{.....(18)}$$

Combining (16) and (18):

$$\tau \sim \rho v'_y l \frac{dv'_x}{dy} \sim \rho l^2 \left(\frac{dv'_x}{dy} \right) \left(\frac{dv'_x}{dy} \right) \quad \text{.....(19)}$$

Incorporating the proportionality constant in l :

$$\tau = \rho l^2 \left(\frac{dv'_x}{dy} \right) \left(\frac{dv'_x}{dy} \right) = \rho l^2 \left(\frac{v'_x}{y} \right)^2 \quad \text{.....(20)}$$

A correlation is now apparent between the mixing length and the eddy viscosity ϵ , which is by definition:

$$\epsilon = \frac{\tau}{\frac{dv'_x}{dy}} = \rho l^2 \left(\frac{dv'_x}{dy} \right) \quad \text{.....(21)}$$

By combining Prandtl's equation with the general linear stress distribution law (for a circular conduit) a velocity distribution equation is obtained:

$$\tau = \tau_0 (1 - y/r_0) = \rho l^2 \left(\frac{\partial v_x}{\partial y} \right)^2 \dots\dots (22)$$

$$l \frac{\partial v_x}{\partial y} = \sqrt{\frac{\tau_0}{\rho}} \cdot \sqrt{1 - \frac{y}{r_0}} \dots\dots (23)$$

Since $\frac{\tau_0}{\rho} = \frac{\rho}{2} V^2$, the dimension of $\sqrt{\frac{\tau_0}{\rho}}$ is velocity. Hence Prandtl termed this group the friction velocity, u_* :

$$u_* = \sqrt{\frac{\tau_0}{\rho}} \dots\dots (24)$$

Although Prandtl's concept serves as a basis for physical understanding, it is not rigorous. Taylor attempted to improve the concept by considering vorticity transfer rather than momentum transfer. Taylor obtained:

$$-\frac{\partial p}{\partial x} = \rho \nu_y l \frac{\partial w_z}{\partial y} = \rho \nu_y l \frac{\partial^2 \bar{v}_x}{\partial y^2} \dots\dots (25)$$

where w_z represents the vorticity fluctuation and l denotes the transverse path in the vorticity transfer.

The Work of Von Karman: In an attempt to further study the pattern of turbulent flow, Karman introduced the velocity deficiency concept. The

velocity deficiency is the difference between the maximum velocity of the flow pattern and the actual velocity at any point.

Karman reasoned that the deficiency velocity should be a function of the friction velocity and the relative distance only:

$$u_d = u_m - u = u_* \cdot f\left(\frac{y}{l_0}\right) = \sqrt{\frac{\tau_0}{\rho}} \cdot f\left(\frac{y}{l_0}\right)$$

or;

$$\frac{u_m - u}{u_*} = f\left(\frac{y}{l_0}\right) \quad \dots\dots\dots(26)$$

He further reasoned that the flow pattern was such that at any two points the factors responsible for turbulence would be similar and differ only in scales. For scales he selected Prandtl's mixing length as the length factor, and since the time scale is dependent on the velocity scale, he selected the successive deviations of the velocity profile as representative of the other factor. He thus arrived at the relation:

$$l = \kappa \left(\frac{\frac{\partial v'_x}{\partial y}}{\frac{\partial^2 v'_x}{\partial y^2}} \right) \quad \dots\dots\dots(27)$$

substituting equation (20),

$$\tau = \rho l^2 \left(\frac{\partial v'_x}{\partial y} \right)^2 \quad \dots (20)$$

combining with equation (22) for a circular pipe,

$$\tau = \tau_0 \left(1 - \frac{y}{r_0} \right) = \rho k^2 \left[\frac{\left(\frac{\partial v'_x}{\partial y} \right)^4}{\left(\frac{\partial^2 v'_x}{\partial y^2} \right)^2} \right] \quad \dots (28)$$

rearranging and substituting $u_* = \sqrt{\frac{\tau_0}{\rho}}$

$$\frac{\frac{\partial^2 v'_x}{\partial y^2}}{\left(\frac{\partial v'_x}{\partial y} \right)^2} = - \frac{k}{u_*} \cdot \frac{1}{\sqrt{1 - \frac{y}{r_0}}} \quad \dots (29)$$

which upon integration gives the equation for the velocity deficiency in a circular pipe:

$$\frac{u_m - u}{u_*} = - \frac{1}{k} \left[\ln \left(1 - \sqrt{1 - \frac{y}{r_0}} \right) + \sqrt{1 - \frac{y}{r_0}} \right] \quad \dots (30)$$

Karman later made a more rigorous analysis and obtained the following relation:

$$- \frac{\partial}{\partial y} \left[v'_y \left(\frac{\rho v'^2}{2} + p \right) \right] + \bar{\tau} \frac{\partial \bar{v}_x}{\partial y} = \mu \sum_{\substack{m= \\ x,y,z}} \sum_{\substack{n= \\ x,y,z}} \left(\frac{\partial v'_m}{\partial n} \right)^2 \quad \dots (31)$$

$$- \frac{\partial}{\partial y} \left(v'_y \frac{\omega'^2}{2} \right) = \gamma \sum_{\substack{m= \\ x,y,z}} \sum_{\substack{n= \\ x,y,z}} \left(\frac{\partial \omega'_m}{\partial n} \right)^2 \quad \dots (32)$$

Reading from left to right, equation (31) states that minus the net rate of increase in turbulent energy as a result of turbulent convection plus the work done by the apparent shearing stress equals the rate of energy dissipation through viscous action within the eddies.

The left side of equation (32) is a measure of the net rate of increase in eddy vorticity and the right side represents the rate of dissipation of eddy vorticity through viscous shear.

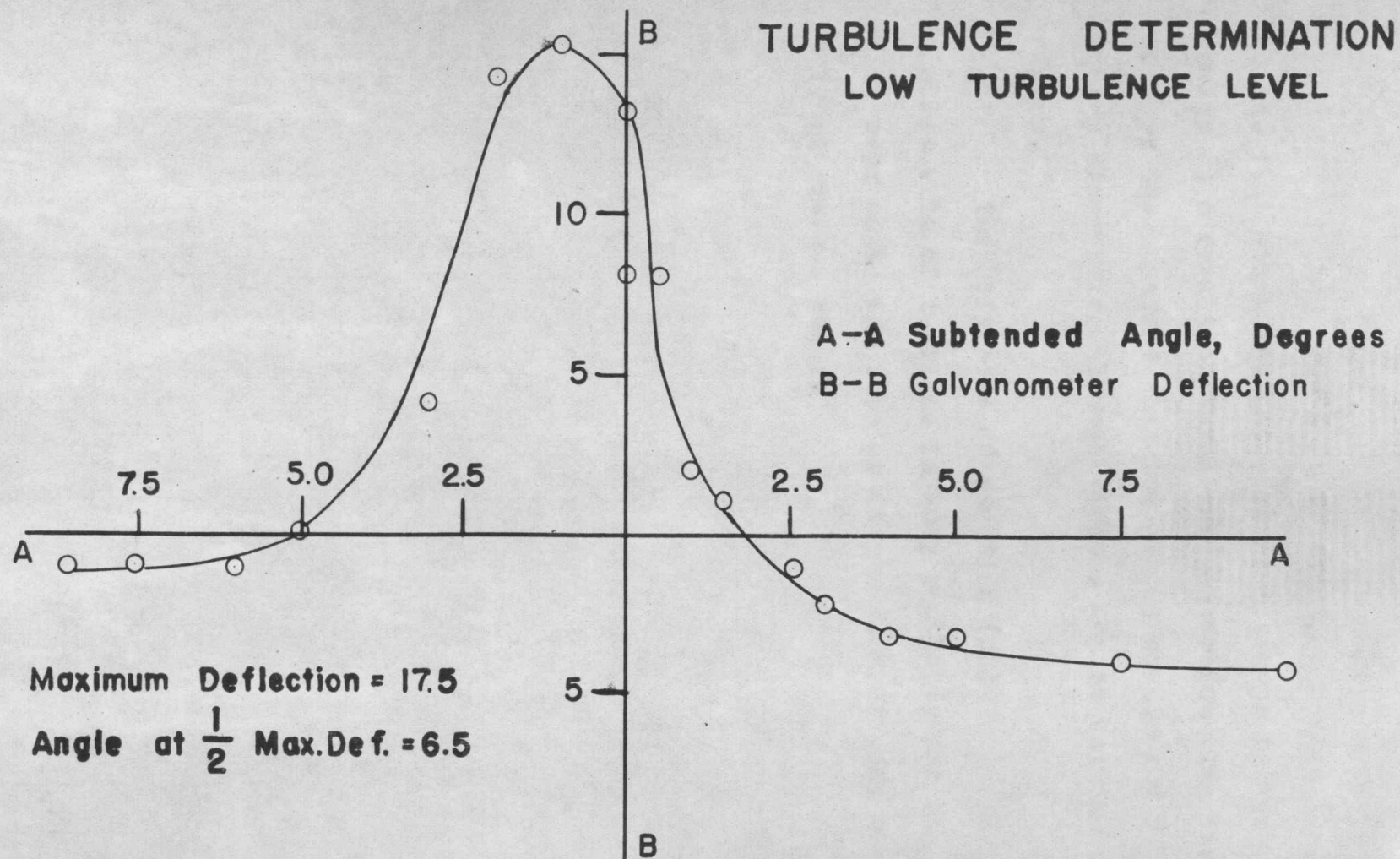


FIGURE 21

TURBULENCE DETERMINATION

HIGH TURBULENCE LEVEL

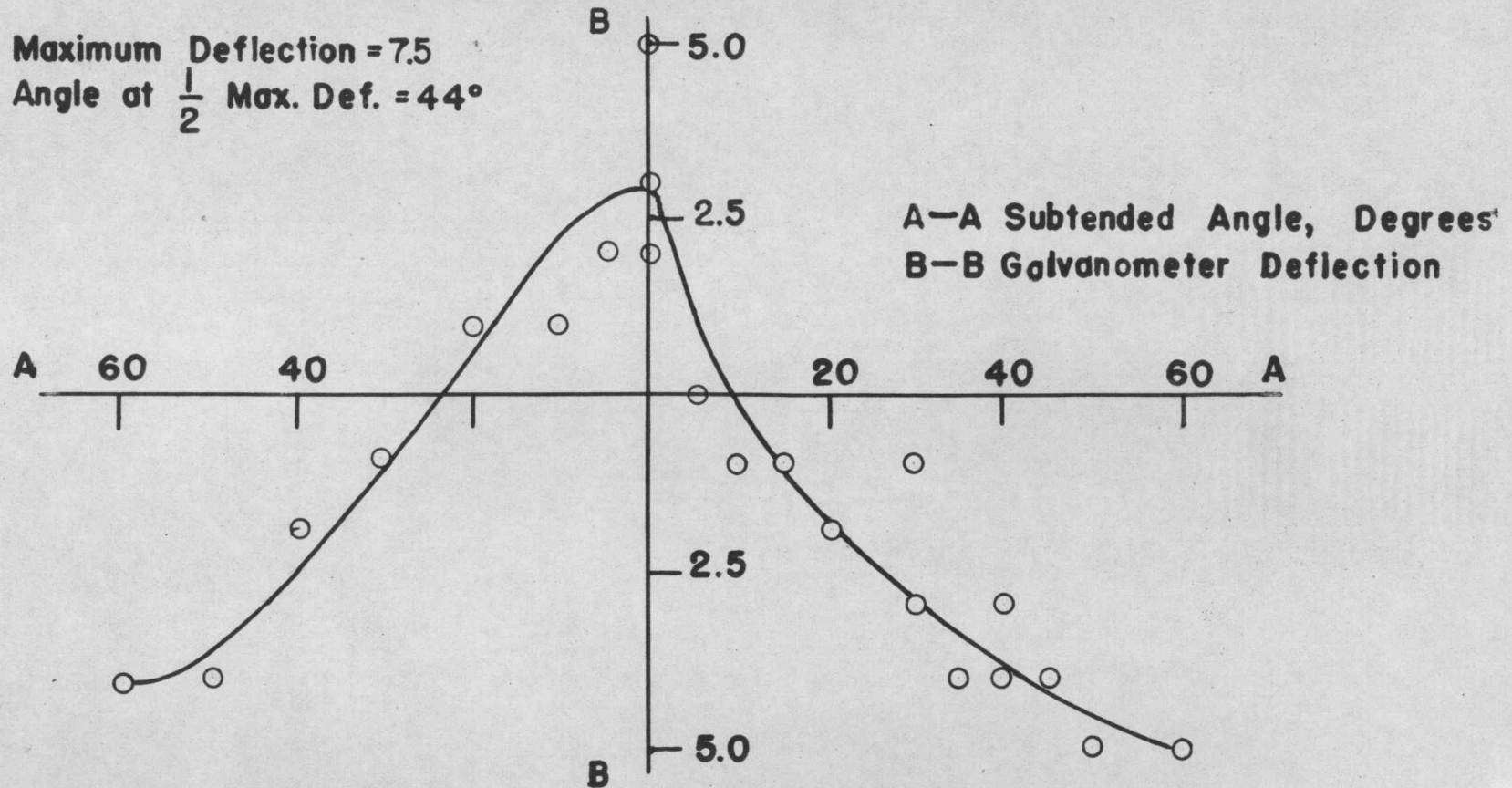


FIGURE 22

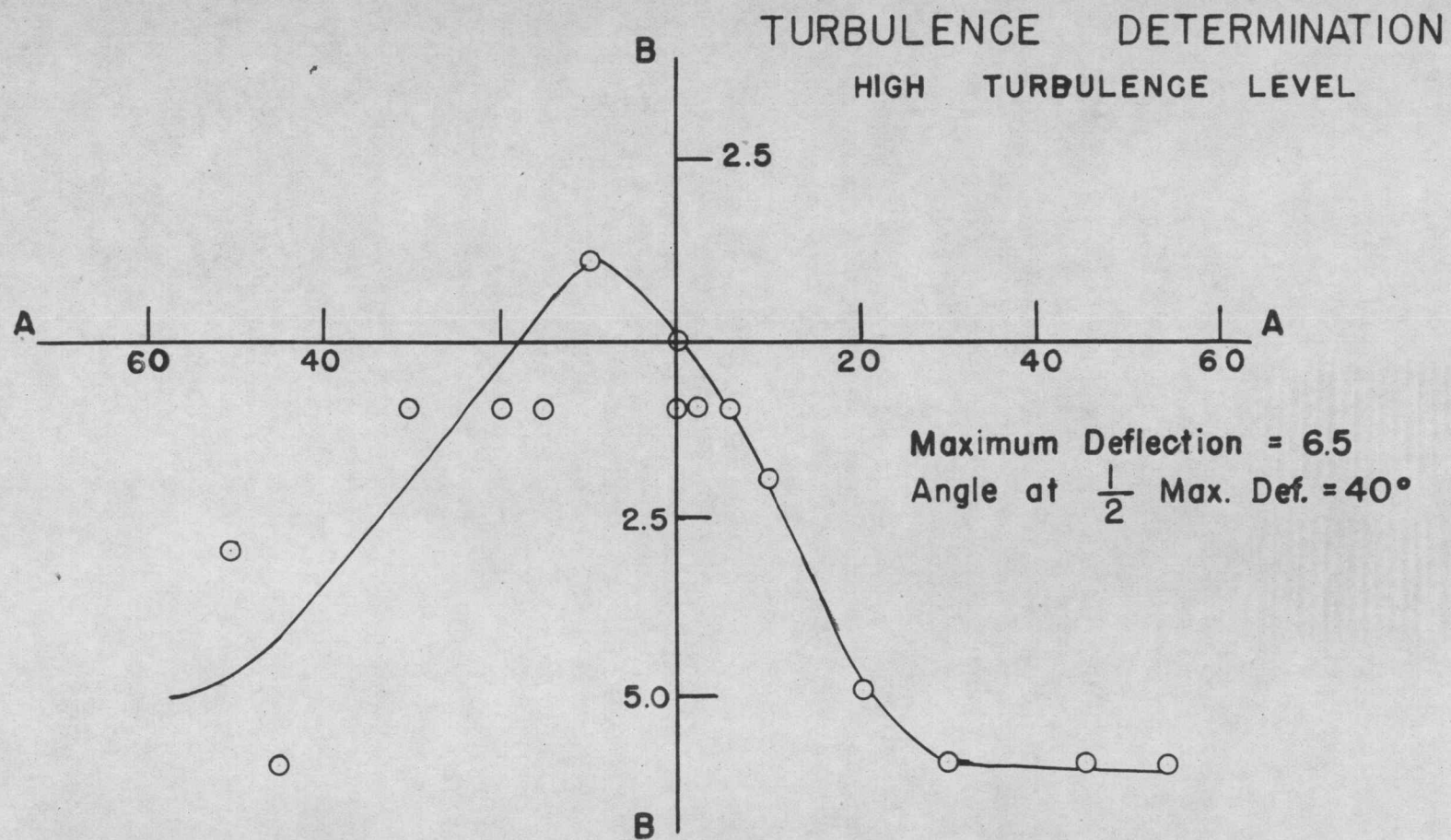


FIGURE 23

A-A Subtended Angle, Degrees
B-B Galvanometer Deflection

BIBLIOGRAPHY

1. Bakhmeteff, Boris A. The mechanics of turbulent flow. Princeton, Princeton University press, 1936. 101 p.
2. Comings, E. W., Clapp, J. T., and Taylor, J. F. Air turbulence and transfer processes. Industrial and Engineering Chemistry. vol. 40, p.p. 1076-1082. (June, 1948).
3. Drew, T. B. and Ryan, W. P. The mechanism of heat transmission: Distribution of heat flow about the circumference of a pipe in a stream of fluid. Transactions of American Institute of Chemical Engineers, vol. 26, pp. 118-147. (1931)
4. Dryden, H. L. and Kuethe, A.M., Effect of turbulence in wind tunnel measurements. Washington, D.C., National advisory committee for aeronautics, Report No. 342. 26 p.
5. Dryden, H. L., Schubauer, G. B., Mock, W. C. Jr., and Skramstad, H. K. Measurements of intensity and scale of wind tunnel turbulence and their relation to the critical Reynolds number of spheres. Washington, D. C., National advisory committee for aeronautics, Report No. 581. 32 p.
6. Rouse, Hunter, Fluid mechanics for hydraulic engineers. New York, McGraw-Hill Co., 1938 422 p.
7. Schubauer, G. B. A turbulence indicator utilizing the diffusion of heat. Washington, D. C. National advisory committee for aeronautics, Report No. 524. 5 p.
8. Small, James The average and local rates of heat transfer from the surface of a hot cylinder in a transverse stream of fluid. Philosophical magazine and Journal of Science. vol. 19 pp. 251-260 (1935)

BIBLIOGRAPHY (Continued)

9. Winding, C. C. and Cheney, A. J. Jr., Mass and heat transfer in tube banks. Industrial and Engineering Chemistry. vol. 40, pp. 1087-1093, (June, 1948).